Temozolomide down-regulates P-glycoprotein in human blood-brain barrier cells by disrupting Wnt3-signalling.

UNIVERSITÀ DEGLI STUDI DI TORINO

Temozolomide down-regulates P-glycoprotein in human blood-brain barrier cells by disrupting Wnt3-signalling.

Chiara Riganti[1,2], Iris C. Salaroglio[1], Martha L. Pinzòn-Daza[1,3], Valentina Caldera[4], Ivana Campia[1], Joanna Kopecka[1], Marta Mellai[4], Laura Annovazzi[4], Pierre-Olivier Couraud[5], Amalia Bosia[1,2], Dario Ghigo[1,2], Davide Schiffer[4]

[1] *Department of Oncology, University of Turin, Via Santena, 5/bis, 10126, Turin, Italy*
[2] *Research Center on Experimental Medicine (CeRMS), University of Turin, Via Santena, 5/bis, 10126, Turin, Italy*
[3] *Unidad de Bioquímica, Facultad de Ciencias Naturales y Matemáticas, Universidad del Rosario, Carrera 6, Bogotá, Colombia*
[4] *Neuro-bio-oncology Center, Policlinico di Monza Foundation, Via Pietro Micca 29, 13100, Vercelli, Italy*
[5] *Institut Cochin, Centre National de la Recherche Scientifique UMR 8104, Institut National de la Santé et de la Recherche Médicale (INSERM) U567, Université René Descartes, 22 rue Méchain, 75014 Paris, France*

Corresponding author: Dr. Chiara Riganti, Department of Oncology, University of Turin, Via Santena 5/bis, 10126 Turin, Italy - Phone: +39-11-6705857; fax: +39-11-6705845; e-mail: chiara.riganti@unito.it

Abstract
Low delivery of many anticancer drugs across the blood-brain barrier (BBB) is a limitation to the success of chemotherapy in glioblastoma. This owes to high levels of ATP-binding cassette transporters like P-glycoprotein (Pgp/ABCB1), which effluxes drugs back to the bloodstream. Temozolomide is one of the few agents able to cross BBB; its effects on BBB cells permeability and Pgp activity are not known.
We found that temozolomide, at therapeutic concentration, increased the transport of Pgp substrates across human brain microvascular endothelial cells and decreased the expression of Pgp. By methylating the promoter of *Wnt3* gene, temozolomide lowers the endogenous synthesis of Wnt3 in BBB cells, disrupts the Wnt3/glycogen synthase kinase 3/β-catenin signalling and reduces the binding of β-catenin on the promoter of *mdr1* gene, which encodes for Pgp. In co-culture models of BBB cells and human glioblastoma cells, pre-treatment with temozolomide increases the delivery, cytotoxicity and antiproliferative effects of doxorubicin, vinblastine and topotecan, three substrates of Pgp which are usually poorly delivered across BBB.
Our work suggests that temozolomide increases the BBB permeability of drugs that are normally effluxed by Pgp back to the bloodstream. These findings may pave the way to new combinatorial chemotherapy schemes in glioblastoma.

Keywords:
blood-brain barrier; temozolomide; P-glycoprotein; Wnt3; glioblastoma multiforme

Abbreviations:

GBM, glioblastoma multiforme;

CNS, central nervous system;

BBB, blood-brain barrier;

TMZ, temozolomide;

ABC, ATP-binding cassette;

BAT, brain-adjacent to tumor;

Pgp, P-glycoprotein;

MRP, multidrug resistance related protein;

BCRP, breast cancer resistance protein;

LRP, low density lipoprotein receptor related protein;

GSK3, glycogen synthase kinase 3;

TCF/LEF, T-cell factor/lymphoid enhancer factor;

Dkk-1, Dickkopf-1;

HBMECs, human brain microvascular endothelial cells;

FCS, fetal calf serum;

BSA, bovine serum albumin;

FITC, fluorescein isothiocyanate;

ZO-1, zonula occludens-1;

TBP, TATA-box binding protein;

qRT-PCR ,Quantitative Real Time-PCR;

ChIP, Chromatin Immunoprecipitation;

MSP, Methylation Specific PCR;

DAPI, 4′,6-diamidino-2-phenylindole dihydrochloride;

LDH, lactate dehydrogenase.

Introduction

Glioblastoma multiforme (GBM) accounts for 65% of primary central nervous system (CNS) tumors in the adult population. Adjuvant chemotherapy is, along with maximal surgical resection and radiation therapy, a standard therapeutic approach in disseminated GBM that almost universally fails [1]. The failure of this approach owes to the highly invasive phenotype of GBM, its strong chemoresistance and the low delivery of anti-neoplastic drugs across the blood-brain barrier (BBB) [1]. First-line therapy in GBM is the systemic administration of the alkylating agent temozolomide (TMZ, Online Resource 1), one of the few drugs to show good permeability across BBB [2]. In systemic circulation, TMZ is rapidly converted into its active metabolite 3-methyl-(triazen-1-yl)imidazole-4-carboxamide (MTIC, Online Resource 1) [3], the chemical entity that likely reaches BBB *in vivo*. Therapeutic protocols currently in use [4] aim either to increase the cumulative dose of TMZ or prolong the duration of the treatment. Until now, however, no treatment protocol has been curative [1]. Since the prognosis of GBM is still poor, alternative approaches have been the object of intensive investigation [2]. The topoisomerase I inhibitors irinotecan and topotecan have shown excellent anti-tumor activity *in vitro* and significant efficacy *in vivo* when administered with TMZ or bevacizumab [5]. Topotecan, however, does not cross the BBB and achieves maximal efficacy only when administered by convection-enhanced delivery [6]. Doxorubicin is highly effective against GBM cells *in vitro*, as well, but its clinical use is limited by low delivery across BBB [7].

The greatest hurdle for many promising anti-GBM drugs is the BBB, the peculiar brain microvascular endothelium, devoid of fenestrations and pinocytic vesicles, and rich in tight junctions, adherent junctions and drug efflux transporters of the ATP-binding cassette (ABC) family [8]. The BBB is disrupted in the core of GBM, but is intact in the "brain-adjacent to tumor" (BAT) area, where invasive GBM cells lay scattered in the non-transformed brain parenchyma. BAT is a critical zone for targeting chemotherapy, because it contains cells that will either spread to other areas of the CNS or cause local relapse. Since the BAT is surrounded by a competent BBB, the delivery of chemotherapeutic drugs to this area is marginal [8]. Alternative strategies – such as the osmotic opening of tight junctions with mannitol [9] or ultrasound [10] – have been devised *in vivo*, to overcome the low permeability of the BBB, with some success. Inhibitors of the ABC transporters present on the luminal side of BBB cells, such as P-glycoprotein (Pgp/ABCB1), multidrug resistance related protein 1 (MRP1/ABCC1) and breast cancer resistance protein (BCRP/ABCG2) [8], have also been used [11]. To date, however, no safe or satisfactory strategies to bypass the ABC transporter-mediated drug efflux have been devised.

Pgp/ABCB1 transports a number of chemotherapeutic agents, such as anthracyclines, taxanes, vinca alkaloids, teniposide/etoposide, topotecan, methotrexate, imatinib, dasatinib, lapatinib, gefitinib, sorafenib, erlotinib and mediates the efflux of several analgesics, anti-epileptics, anti-retrovirals, antibiotics [8]. In BBB cells Pgp/ABCB1 is up-regulated by

different stimuli, such as tumor necrosis factor α [12] and ligands of pregnane X receptor, constitutive androstane receptor [13], aryl hydrocarbon receptor [14].

Recent data show that the activation of the Wnt-canonical pathway, critical for angiogenesis in brain [15] and the acquisition of BBB properties [16], up-regulates Pgp/ABCB1 in human BBB cells [17, 18]. In the Wnt-canonical pathway, the binding of soluble Wnt proteins on Frizzled receptor and low-density-lipoprotein receptor related protein-5 and -6 (LRP5/LRP6) co-receptors decreases the activity of the enzyme glycogen synthase kinase 3 (GSK3). By doing so, Wnt allows β-catenin to move from the cytosolic APC/axin complex into the nucleus, where it binds to the T-cell factor/lymphoid enhancer factor (TCF/LEF) and induces the transcription of target genes, such as *mdr1*, which encodes for Pgp/ABCB1 [19].

While several determinants have been reported to up-regulate Pgp/ABCB1 in BBB cells, determinants that down-regulate Pgp/ABCB1 are poorly known. There is some evidence that specific polymorphisms of Pgp/ABCB1 change the delivery of TMZ across BBB [20], but the relation between TMZ and Pgp/ABCB1 is still controversial. In this study we asked the question whether a clinically achievable dose of TMZ can affect the permeability and the activity/expression of ABC transporters in human BBB cells. We found that TMZ specifically down-regulates Pgp/ABCB1 by interfering with the Wnt/GSK3/β-catenin signalling.

Materials and methods

Chemicals. Plasticware for cell cultures was from Falcon (Becton Dickinson, Franklin Lakes, NJ). TMZ, doxorubicin, mitoxantrone, vinblastine, topotecan were obtained by Sigma Chemical Co (St. Louis, MO). WntA [2-amino-4-(3,4-(methylenedioxy)benzylamino)-6-(3-methoxyphenyl)pyrimidine] was purchased from Calbiochem (San Diego, CA). Human recombinant Dickkopf-1 (Dkk-1) was from R&D Systems (Minneapolis, MN). Electrophoresis reagents were obtained from Bio-Rad Laboratories (Hercules, CA); the protein content of cell lysates was assessed with the BCA kit from Sigma Chemical Co. When not otherwise specified, all the other reagents were purchased from Sigma Chemical Co.

Cells.

The immortalized hCMEC/D3 cells, a primary human brain microvascular endothelial cell line that retains the BBB characteristics *in vitro*, were cultured as reported [21]. Cells were seeded at 50,000/cm² density and were grown for 7 days up to confluence in Petri dishes and Transwell (0.4 μm diameter pores-size, Corning Life Sciences, Chorges, France). Primary human brain microvascular endothelial cells (HBMECs) were purchased from PromoCell GmbH (Heidelberg, Germany) and cultured in the Endothelial Cell Growth Medium MV (PromoCell GmbH), supplemented with 5% v/v fetal

calf serum (FCS), 0.4% v/v Endothelial Cell Growth Supplement (PromoCell GmbH), 10 ng/mL EGF, 90 µg/mL heparin, 1 µg/mL hydrocortisone.

Primary human GBM cells (CV17, 01010627) were obtained from surgical samples of patients from the Department of Neuroscience, Neurosurgical Unit, University of Turin, Italy. The pathological diagnosis was performed according to WHO guidelines. Cells were cultured in DMEM-F12 medium, supplemented with 1 mol/L HEPES, 0.3 mg/mL glucose, 75 µg/mL $NaHCO_3$, 2 mg/mL heparin, 2 mg/mL bovine serum albumin (BSA), 2 mmol/L progesterone, 20 ng/mL EGF, 10 ng/mL bFGF. U87-MG cells (ATCC, Rockville, MD) were used as GBM reference cell line and cultured as reported above.

In co-culture experiments, 500,000 (for intracellular doxorubicin accumulation, PCR and cytotoxicity assays) or 1,000 (for proliferation assay) GBM cells were added in the lower chamber of Transwell 4 days after seeding hCMEC/D3 cells or HBMECs in Transwell inserts. After 3 days of co-culture the medium of the upper chamber was replaced with fresh medium with or without TMZ, doxorubicin, vinblastine or topotecan, alone or in combination as detailed below.

Permeability coefficient across the BBB cells.

The permeability to dextran-fluorescein isothiocyanate (FITC; molecular weight 70 kDa), [^{14}C]-sucrose (589 mCi/mmol; PerkinElmer, Waltham, MA), [^{14}C]-inulin (10 mCi/mmol; PerkinElmer) was taken as a parameter of tight junction integrity [21, 22]. The permeability to doxorubicin, [^{3}H]-vinblastine (0.25 mCi/mL, PerkinElmer), mitoxantrone, was taken as index of ABC transporters activity [21]. hCMEC/D3 cells, seeded at 50,000/cm² and grown for 7 days up to confluence in 6-multiwell Transwell inserts, were incubated at day 4 with or without TMZ (50 µmol/L for 72 h). Then the culture medium was replaced in both chambers; 2 µmol/L dextran-FITC, 2 µCi/mL [^{14}C]-sucrose, 2 µCi/mL [^{14}C]-inulin, 5 µmol/L doxorubicin, 2 µCi/mL [^{3}H]-vinblastine, 10 µmol/L mitoxantrone were added to the upper chamber of Transwell. After 3 h the medium in the lower chamber was collected. The amount of [^{14}C]-sucrose, [^{14}C]-inulin or [^{3}H]-vinblastine was measured using a Tri-Carb Liquid Scintillation Analyzer (PerkinElmer). Radioactivity was converted in nmol/cm^2, using a calibration curve previously prepared. The amount of dextran-FITC, doxorubicin and mitoxantrone present in the lower chamber was measured fluorimetrically, using a LS-5 spectrofluorimeter (PerkinElmer). Excitation and emission wavelengths were: 494 nm and 518 nm (dextran-FITC); 475 nm and 553 nm (doxorubicin); 607 nm and 684 nm (mitoxantrone). Fluorescence was converted in nmol/cm^2, using a calibration curve previously set. The permeability coefficients were calculated as reported [23]. In time- and temperature-dependence experiments, the Transwell inserts were incubated at 4°C, 15°C and 37°C, and treated as reported above; aliquots of the medium from the lower chamber were collected every 30 min up to 3 h. The amount of doxorubicin or vinblastine in the lower chamber was quantified as described earlier. When indicated, a 25% w/v solution of mannitol, used to increase the leakage of solutes through the BBB

tight junctions, was co-incubated in the upper chamber.

For TMZ permeability, hCMEC/D3 cells seeded in Transwell inserts as reported above were incubated for 72 h with 0.7 μC/mL [^{3}H]-TMZ (Moravek Biochemical Inc., Brea, CA), equivalent to 10 μmol/L TMZ, in the presence of increasing concentrations (50, 100, 200 μM) of cold TMZ. After this incubation period, the amount of [^{3}H]-TMZ in the lower chamber was measured by liquid count scintillation. The results were expressed as the percentage of [^{3}H]-TMZ recovered in the lower chamber after 72 h versus [^{3}H]-TMZ added in the upper chamber at time 0, taking into account the concentration of cold TMZ added in the upper chamber at time 0.

Rhodamine 123 and Hoechst 33342 accumulation.

hCMEC/D3 cells were grown up to confluence in Petri dishes and incubated in the absence or presence of TMZ, as reported above. Cells were washed with PBS, detached with Cell Dissociation Solution (Sigma), centrifuged at 13,000 x g for 5 min and re-suspended in 0.5 mL culture medium containing 5% v/v FCS. A 50 μL aliquot was taken away, sonicated and used for the measurement of the protein content. 20 μmol/L rhodamine 123 or 50 μmol/L Hoechst 33342 were added to the remaining sample. After 10 min at 37°C, cells were washed three times with PBS and re-suspended in 1 mL PBS. The intracellular fluorescence of rhodamine 123 (index of Pgp/ABCB1 and MRP1/ABCC1 activity) and Hoecst 33342 (index of BCRP/ABCG2 activity) was measured fluorimetrically, using a LS-5 spectrofluorimeter (PerkinElmer). Excitation and emission wavelengths were: 488 nm and 520 nm for rhodamine 123, 370 nm and 450 nm for Hoechst 33342. Fluorescence was converted in nmol/mg cell proteins, using a calibration curve previously set.

Western blot analysis.

Cells were rinsed with lysis buffer (50 mmol/L Tris, 10 mmol/L EDTA, 1% w/v Triton-X100), supplemented with the protease inhibitor cocktail set III (80 μmol/L aprotinin, 5 mmol/L bestatin, 1.5 mmol/L leupeptin, 1 mmol/L pepstatin; Calbiochem), 2 mmol/L phenylmethylsulfonyl fluoride and 1 mmol/L sodium orthovanadate, then sonicated and centrifuged at 13,000 x g for 10 min at 4^{o}C. 20 μg of protein extracts were subjected to SDS-PAGE and probed with the following antibodies: anti-claudin 3 (Invitrogen Life Technologies, Monza, Italy); anti-claudin 5 (Invitrogen Life Technologies); anti-occludin (Invitrogen Life Technologies); anti-zonula occludens-1 (ZO-1; Invitrogen Life Technologies); anti-Pgp/ABCB1 (clone C219, Cabiochem), anti-MRP1/ABCC1 (Abcam, Cambridge, MA), anti-BCRP/ABCG2 (Santa Cruz Biotechnology Inc, Santa Cruz, CA), anti-Wnt3 (Abcam); anti-GSK3 (BD Biosciences, Franklin Lakes, NJ); anti-phospho(Tyr216)GSK3 (BD Biosciences); anti-β-catenin (BD Biosciences); anti-phospho(Ser33/37/Thr41)β-catenin (Cell Signalling Technology Inc., Danvers, MA); anti-β-tubulin (Santa Cruz Biotechnology Inc.) This procedure was followed by the exposure to a

peroxidase-conjugated secondary antibody (Bio-Rad). The membranes were washed with Tris buffer saline-Tween 0.1% v/v, and proteins were detected by enhanced chemiluminescence (PerkinElmer).

Cytosol/nucleus separation was performed as reported [24]. 10 μg of cytosolic or nuclear extracts were subjected to Western blot analysis using the anti-β-catenin antibody. To check the equal control loading in cytosolic and nuclear fractions, samples were probed respectively with an anti-β-tubulin or an anti-TATA-box binding protein (TBP/TFIID) antibody (Santa Cruz Biotechnology Inc). To exclude any cytosolic contamination of nuclear extracts or *vice-versa*, we verified that β-tubulin was undetectable in nuclear samples and TBP was undetectable in cytosolic samples.

The densitometric analysis of Western blots was performed with the ImageJ software (http://rsb.info.nih.gov/ij/) and expressed as arbitrary units, where '1 unit' is the mean band density in untreated cells.

Quantitative Real Time-PCR (qRT-PCR).

Total RNA was extracted and reverse-transcribed using the QuantiTect Reverse Transcription Kit (Qiagen, Hilden, Germany). qRT-PCR was carried out using IQ^{TM} SYBR Green Supermix (Bio-Rad), according to the manufacturer's instructions. The same cDNA preparation was used to quantify the genes of interest and the housekeeping gene β-actin. Primer sequences, designed with the Primer3 software (http://frodo.wi.mit.edu/primer3), are reported in the Online Resource 2. The relative quantification was performed by comparing each PCR product with the housekeeping PCR product, using the Bio-Rad Software Gene Expression Quantitation (Bio-Rad).

Chromatin Immunoprecipitation (ChIP).

ChIP experiments were performed using the Magna ChIP™ A/G Chromatin Immunoprecipitation Kit (Millipore, Billerica, MA). Samples were immunoprecipitated with 5 μg of anti-β-catenin antibody or with no antibody. The immunoprecipitated DNA was washed and eluted twice with 100 μl of elution buffer (0.1 M $NaHCO_3$, 1% w/v SDS), the cross-linking was reversed by incubating the samples at 65°C for 6 h. Samples were then treated with 1 μl proteinase K for 1 h at 55°C. The DNA was eluted in 50 μl of H_2O and analyzed by PCR. The putative β-catenin site on *mdr1* promoter was validated by the MatInspector software (http://www.genomatix.de/). Primers sequences, designed with the Primer3 software (http://frodo.wi.mit.edu/primer3), are reported in the Online Resource 2. PCR products were visualized on a 3% agarose gel, stained with 0.05% v/v ethidium bromide. As negative control, immunoprecipitated samples were subjected to PCR with primers matching a region 10,000 bp upstream the *mdr1* promoter. In this condition no PCR product was detected (not shown).

Flow cytometry analysis.

Cells were washed with PBS, detached with Cell Dissociation Solution and re-suspended at 5×10^5 cells/mL in 1 mL of

culture medium containing 5% v/v FCS. Samples were washed with 0.25% w/v BSA-PBS, incubated with the primary antibody for Frizzled (Santa Cruz Biotechnology Inc.) or LRP6 (Abcam) for 45 min at 4°C, then washed twice and incubated with secondary FITC-conjugated antibody for 30 min at 4°C. After washing and fixing in paraformaldehyde 2% w/v, the surface amount of Frizzled or LRP6 was detected on 100,000 cells by a FACSCalibur system, using the Cell Quest software (Becton Dickinson). Control experiments included incubation of cells with non-immune isotypic antibody, followed by the secondary antibody.

Promoter methylation assay.

1 µg of genomic DNA was subjected to bisulphite modification using the Methyl Easy Xceed kit (Human Genetics Signatures, Randwick, Australia), following the manufacturer's instruction. *Wnt3* promoter sequence was obtained using the UCSC Genome Browser (http://genome.ucsc.edu/). The CpG islands localization on *Wnt3* promoter and the design of primers for Methylation Specific PCR (MSP) was performed with the Methprimer software (http://www.urogene.org/methprimer). Primers specific for methylated and unmethylated *Wnt3* promoter are reported in the Online Resource 2. MSP was performed with AmpliTaq Gold DNA Polymerase (Applied Biosystems, Carlsbad, CA), including universally methylated (CpGenome, Millipore) and unmethylated DNA samples (Human Genetics Signatures) as control. PCR products were visualized on a 3% w/v agarose gel, stained with 0.05% v/v ethidium bromide.

Generation of Wnt3-silenced cells.

300,000 hCMEC/D3 cells were treated with Turbofectin 8.0 (Origene Technologies Inc, Rockville, MD) and 1 µg of 29mer shRNA Wnt3 construct in pGFP-C-shLenti-vector (Origene Technologies Inc.) or non-targeting 29-mer scrambled shRNA cassette in pGFP-C-shLenti Vector (Origene Technologies Inc.), used as control. 24 h after the transfection, the green fluorescent cells were sorted by flow cytometry analysis. 48 h after the transfection, the cells were transferred in puromycin-containing medium, to select clones stably silenced for Wnt3. The silencing efficacy was controlled every 2 passages by qRT-PCR and Western blot analysis of Wnt3.

Intracellular doxorubicin accumulation in co-culture models.

After 3 days of co-culture, 5 µmol/L doxorubicin for 24 h or 50 µmol/L TMZ for 72 h plus 5 µmol/L doxorubicin in the last 24 hours were added to the upper chamber of Transwell inserts containing hCMEC/D3 cells monolayer. Then the GBM cells were collected from the lower chamber, rinsed with PBS, re-suspended in 0.5 mL ethanol/HCl 0.3 N (1:1 v/v) and sonicated. A 50 µL aliquot was used to measure the protein content and the remaining sample was used to quantify fluorimetrically the intracellular doxorubicin content as described above. Results were expressed as nmol doxorubicin/mg cell proteins.

For fluorescence microscope analysis, the GBM cells in the lower chamber were seeded on sterile glass coverslips and treated as reported above. At the end of the incubation period, cells were rinsed with PBS, fixed in 4% w/v paraformaldehyde for 15 min, washed three times with PBS and incubated with 4′,6-diamidino-2-phenylindole dihydrochloride (DAPI) for 3 min at room temperature in the dark. Cells were washed three times with PBS and once with water, then the slides were mounted with 4 µl of Gel Mount Aqueous Mounting and examined with a Leica DC100 fluorescence microscope (Leica Microsystems GmbH, Wetzlar, Germany). For each experimental point, a minimum of 5 microscopic fields were examined.

Cytotoxicity assays in co-culture models.

After 3 days of co-culture, the upper chamber of the Transwell inserts containing hCMEC/D3 cells was filled with fresh medium or with medium containing: 50 µmol/L TMZ for 72 h, 5 µmol/L doxorubicin for 24 h, 50 µmol/L TMZ for 72 h plus 5 µmol/L doxorubicin in the last 24 h, 20 nmol/L vinblastine for 24 h, 50 µmol/L TMZ for 72 h plus 20 nmol/L vinblastine in the last 24 h, 10 µmol/L topotecan for 24 h, 50 µmol/L TMZ for 72 h plus 10 µmol/L topotecan in the last 24 h. According to preliminary experiments, 50 µmol/L TMZ for 72 h did not produce any significant toxicity in GBM cells or in hCMEC/D3 cells. The concentration of doxorubicin, vinblastine and topotecan was chosen on the basis of previous works, showing that at these concentrations each drug reduced the survival of GBM cells – in the absence of BBB cells – to less than 20% [25-27].

The release of lactate dehydrogenase (LDH) in cell supernatant, used as an index of cell damage and necrosis, was measured spectrophotometrically as described earlier [28]. Results were expressed as percentage of extracellular LDH versus total (intracellular plus extracellular) LDH. The activation of caspase 3, as index of apoptosis, was assessed in cells lysates as reported [29]. The amount of the hydrolyzed DEVD-7-amino-4-methylcumarine, a substrate of caspase 3, was measured fluorimetrically. Results were expressed as nmol/mg cell protein using a calibration curve prepared with standard solutions of amino-4-methylcumarine.

Proliferation assays in co-culture models.

1,000 GBM cells were seeded in the lower chamber of Transwell, containing confluent hCMEC/D3 cells in the insert. This time was considered “day 0” in the proliferation assay. After 3 days of co-culture, the upper chamber of the Transwell inserts was filled with fresh medium or medium containing: 50 µmol/L TMZ for 72 h, 5 µmol/L doxorubicin for 24 h, 50 µmol/L TMZ for 72 h plus 5 µmol/L doxorubicin in the last 24 h, 20 nmol/L vinblastine for 24 h, 50 µmol/L TMZ for 72 h plus 20 nmol/L vinblastine in the last 24 h, 10 µmol/L topotecan for 24 h, 50 µmol/L TMZ for 72 h plus 10 µmol/L topotecan in the last 24 h. The treatments were repeated every 7 days, for 4 weeks. At day 7, 14, 21, 28 GBM cells were

collected, transferred into a 96-wells plate, fixed with 4% w/v paraformaldehyde and stained with 0.5% w/v crystal violet solution for 10 min at room temperature. The plate was washed three times in water, then 100 µL of 0.1 mmol/L sodium citrate in 50 % v/v ethanol was added to each well and the absorbance was read at 570 nm. The absorbance units were converted into cell number, according to a titration curve obtained with serial cells dilutions of each cell line. To check that hCMEC/D3 cells retain BBB properties, the permeability to dextran and inulin was measured weekly in a parallel set of Transwell. No significant changes in the permeability coefficients were detected during the whole experiment (data not shown).

Statistical analysis.

All data in text and figures are provided as means ± SD. The results were analyzed by a one-way Analysis of Variance (ANOVA). A $p < 0.05$ was considered significant.

Results

Temozolomide increases the transport of Pgp/ABCB1 substrates through hCMEC/D3 BBB cells monolayer.

We investigated whether 50 µmol/L TMZ (equivalent to 9.7 µg/mL, a concentration that is clinically achievable in blood) [30] may affect the transport of other molecules through hCMEC/D3 monolayer.

As shown in Figure 1a (upper panels), the permeability of molecules which have a paracellular diffusion in case of tight junctions leakage, such as dextran, inulin and sucrose widely varied in hCMEC/D3 cells, but was compatible with intact tight junctions [21]. The permeability coefficients followed this rank order: inulin > sucrose > dextran 70. TMZ did not affect the permeability of these compounds (Figure 1a, upper panels). Also the permeability of ABC transporters substrates displayed major differences: among the substrates of Pgp/ABCB1 and MRP1/ABCC1 proteins, doxorubicin was almost 100-fold less transported than vinblastine across the hCMEC/D3 monolayer. When we analyzed the transport of doxorubicin and vinblastine at earlier time points, it increased linearly in a temperature- and time-dependent manner (Online Resource 3a). In the presence of mannitol, an agent that disrupts the tight junctions as shown by the increased permeability of inulin (Online Resource 3b), we did not detect significant changes in doxorubicin and vinblastine transport (Online Resource 3c). These results suggest that paracellular leakage contributed minimally to the transport of doxorubicin and vinblastine across the hCMEC/D3 monolayer. Because of their high hydrophobicity, doxorubicin and vinblastine are expected to enter by passive diffusion [31, 32], and then to be effluxed back by Pgp/ABCB1 and MRP1/ABCC1. Of note, the permeability of doxorubicin and vinblastine was significantly higher in hCMEC/D3 cells pre-treated with TMZ (Figure 1a, lower panels). By contrast, the permeability of mitoxantrone, a substrate of BCRP/ABCG2 with a permeability

coefficient between doxorubicin and vinblastine in hCMEC/D3 cells, was unaffected by TMZ (Figure 1a, lower panels). Congruent with these results, TMZ increased the intracellular accumulation of rhodamine 123, which is effluxed by Pgp/ABCB1 and MRP1/ABCC1, and did not change the accumulation of Hoechst 33342, which is effluxed by BCRP/ABCG2 (Online Resource 4).

When we analyzed the expression of typical tight junctions proteins in cells exposed to TMZ, we detected a small decrease of claudin-3. Claudin-5, occludin and ZO-1 did not change (Figure 1b). hCMEC/D3 cells constitutively expressed Pgp/ABCB1, MRP1/ABCC1 and BCRP/ABCG2 (Figure 1c). Of note, TMZ decreased the amount of Pgp/ABCB1, without affecting the other two proteins (Figure 1c). The decrease of Pgp/ABCB1 exerted by TMZ was dose-dependent (Online Resource 5a). We next measured the transport of [^{3}H]-TMZ across hCMEC/D3 monolayer, in the presence of increasing concentrations of unlabelled TMZ, sufficient to significantly reduce Pgp/ABCB1: as shown in the Online Resource 5b, the amount of [^{3}H]-TMZ in the lower chamber of Transwell was about 100% of the amount added in the upper chamber, independently of the decrease of Pgp/ABCB1 induced by TMZ itself. These results suggest that Pgp/ABCB1 played a minor role in the transport of TMZ across hCMEC/D3 monolayer and that TMZ did not enhance its own delivery by decreasing Pgp/ABCB1.

Under our experimental conditions, TMZ (50 μmol/L for 72 h) showed no toxicity on hCMEC/D3 cells, as measured by LDH release (as described below) and caspase-3 activity (not shown).

Temozolomide down-regulates the transcription of *mdr1* gene, by disrupting the Wnt/GSK3/β-catenin pathway in hCMEC/D3 BBB cells.

To clarify the molecular mechanisms by which TMZ decreases Pgp/ABCB1 protein, we asked the questions whether decreased gene transcription could be accountable and which transcription factors could be the targets of the drug. TMZ lowered the mRNA levels of *mdr1* (Figure 2a) and decreased the binding of β-catenin, a known inducer of Pgp/ABCB1 in hCMEC/D3 cells [16], to the *mdr1* promoter (Figure 2b).

In hCMEC/D3 cells β-catenin was detectable in both cytosolic and nuclear extracts under basal conditions (Figure 2c); TMZ decreased the amount of β-catenin present in the nucleus (Figure 2c). In parallel the drug increased the active form of GSK3 - i.e. phospho(Tyr216)GSK3 -, and the amount of serine 33/37/threonine 41-phosphorylated β-catenin (Figure 2d). As a whole, these data suggest that TMZ may reduce the amount of β-catenin active as transcription factor.

In hCMEC/D3 cells the activity of GSK3 is controlled by the Wnt canonical pathway [17, 18].

The presence of Wnt proteins in endothelial cells is restricted to some antigens of the large Wnt family, such as Wnt2b, Wnt3, Wnt4 and Wnt5 [33]. The first three ones are associated to the canonical GSK3/β-catenin pathway [34-36].

We wanted to validate the hypotheses that 1) the Wnt/GSK3/β-catenin axis controls the expression of the *mdr1* gene in hCMEC/D3 and 2) TMZ down-regulates the expression of Pgp/ABCB1 by interfering with this axis. We therefore treated cells with the Wnt activator WntA, the Wnt antagonist Dkk-1 and the GSK3 inhibitor LiCl. As shown in Figure 3a, WntA decreased the phosphorylation of GSK3, whereas Dkk-1 produced the opposite effect. The phosphorylation of β-catenin, which was low in untreated hCMEC/D3 cells, was not significantly reduced by WntA and was increased by Dkk-1. LiCl did not change the phosphorylation of GSK3 on tyrosine 216, but slightly reduced the phosphorylation of β-catenin on serine 33/37/threonine 41, suggesting that it effectively inhibited the activity of GSK3. The nuclear translocation of β-catenin (Figure 3b) and its binding on *mdr1* promoter (Figure 3c) was increased by WntA and LiCl, and reduced by Dkk-1. Indeed, hCMEC/D3 cells treated with Dkk-1 had lower levels of *mdr1* mRNA (Figure 3d) and Pgp/ABCB1 protein (Figure 3e). Cells treated with WntA or LiCl had higher amounts of *mdr1* mRNA and Pgp/ABCB1 protein (Figure 3d-e). Congruent with this trend, Dkk-1 increased, and WntA and LiCl decreased the permeability of doxorubicin, chosen as a Pgp/ABCB1 substrate, across the hCMEC/D3 monolayer (Figure 3f). Interestingly, TMZ mimicked the effects of Dkk-1 and counteracted the effects of WntA and LiCl on β-catenin phosphorylation (Figure 3a), nuclear translocation (Figure 3b) and *mdr1* promoter binding (Figure 3c), on *mdr1* mRNA (Figure 3d) and Pgp/ABCB1 levels (Figure 3e) and on doxorubicin permeability (Figure 3f). These findings suggested that TMZ reduced *mdr1* transcription by inhibiting the Wnt/GSK3/β-catenin axis.

Temozolomide lowers the synthesis of Wnt3 in hCMEC/D3 BBB cells.

TMZ did not change the surface amount of the Wnt receptor Frizzled and Wnt co-receptor LRP6 (Online Resource 6), leading to exclude interference with the Wnt3-signalling on the surface.

We asked the question, then, whether TMZ down-regulated the endogenous synthesis of one or more Wnts proteins. We did not detect Wnt2b and Wnt4 in hCMEC/D3 cells (data not shown). Wnt3 was instead detectable at protein (Figure 4a) and mRNA (Figure 4b) level. Notably, TMZ reduced both Wnt3 protein and mRNA (Figure 4a-4b).

Since TMZ is an alkylating agent that methylates DNA [4], we asked the question whether it might cause the methylation of the *Wnt3* promoter. *Wnt3* promoter has indeed several CpG islands (Online Resource 7), usually methylated in infrequently transcripted genes and unmethylated in highly transcripted ones. MSP PCR assays showed that Wnt3 promoter was fully unmethylated in hCMEC/D3 cells (Figure 4c). TMZ decreased the amount of unmethylated promoter and induced the appearance of a methylated band (Figure 4c), thus appearing to be a good candidate for the epigenetic down-regulation of Wnt3.

To confirm that Wnt3 was a critical controller of *mdr1* expression in our model, we permanently silenced Wnt3 in

hCMEC/D3 cells; silencing produced a 90% reduction in *Wnt3* mRNA (Figure 5a) and made the Wnt3 protein undetectable by Western blotting (Figure 5b). The depletion of the Wnt3 protein significantly increased the amount of phospho(Tyr216)GSK3 and phospho(Ser33/37/Thr41)β-catenin (Figure 5c), prevented the binding of β-catenin on *mdr1* promoter (Figure 5d) and markedly reduced the expression of Pgp/ABCB1 (Figure 5e). Additionally Wnt3-depleted hCMEC/D3 cells showed a higher permeability to doxorubicin than wild-type cells (Figure 5f).

Temozolomide increases the antitumor efficacy of Pgp/ABCB1 substrates in glioblastoma-hCMEC/D3 co-culture models.

Since TMZ decreased the amount and activity of Pgp/ABCB1 in BBB cells, we next asked the question whether the efficacy of anti-cancer drugs commonly effluxed by this transporter would be improved. With this goal in mind, we cultured hCMEC/D3 cells, treated or not with TMZ, in Transwell inserts, containing different GBM cell lines (CV17, 01010627, U87-MG) in the lower chamber. Without pre-treatment with TMZ, doxorubicin was applied in the upper chamber, facing the luminal side of hCMEC/D3 monolayer, which expresses high amounts of Pgp/ABCB1 [37]. As expected, doxorubicin was poorly delivered to GBM cells in the lower chamber (Figure 6a). Pre-treatment of hCMEC/D3 cells with TMZ significantly increased the intratumor amount of doxorubicin (Figure 6a). The typical nuclear red fluorescence of doxorubicin [28] was undetectable in 01010627 GBM cells recovered from the lower chamber of the co-cultures, whereas pre-treatment of hCMEC/D3 cells with TMZ restored the nuclear accumulation of doxorubicin in GBM cells (Figure 6b). Interestingly, TMZ decreased the expression levels of *mdr1* also in the GBM cells cultured in the lower chamber (Online Resource 8), as it did in hCMEC/D3 cells.

Under the experimental conditions used, neither TMZ nor doxorubicin alone induced detectable cytotoxicity, measured as extracellular release of LDH and activation of caspase 3 (Figure 6c), in GBM cells. The TMZ-doxorubicin combination produced cytotoxic effects in all the tumor cell lines analyzed (Figure 6c). The rate of proliferation of the three GBM cell lines was not affected by the addition of doxorubicin in the upper chamber of the Transwell (Figure 6d). TMZ applied in the upper chamber reduced the proliferation rate of all tumor cell lines in a time-dependent way; of note, its antiproliferative effect was significantly enhanced when TMZ was followed by doxorubicin (Figure 6d). Under these conditions TMZ and doxorubicin, alone or in combination, did not induce any significant cytotoxicity (Online Resource 9a) and did not affect cell proliferation (Online Resource 9b) in hCMEC/D3 cells.

The chemosensitizing properties of TMZ were not limited to doxorubicin. In the same co-culture models vinblastine and topotecan, two other substrates of Pgp/ABCB1, did not increase the extracellular LDH (Online Resource 10a), did not

activate the caspase 3 (Online Resource 10b) and did not decrease cell proliferation (Online Resource 10c) of GBM cells, when applied in the upper chamber of the Transwell. Only the pre-treatment of hCMEC/D3 cells with TMZ followed by vinblastine and topotecan exerted significant cytotoxicity (Online Resource 10a-b) and reduced the proliferation (Online Resource 10c) of GBM cells cultured under the BBB monolayer. The combination of TMZ plus vinblastine or TMZ plus topotecan (Online Resource 10c) were significantly more effective in reducing cell proliferation after 21 and 28 days ($p < 0.02$) than TMZ alone (Figure 6d).

Notably, the same permeabilizing effects induced by TMZ in wild-type BBB cells was obtained after Wnt3 depletion: indeed, Wnt3-silenced hCMEC/D3 monolayer allowed a higher delivery (Figure 6e) and toxicity (Figure 6f) of doxorubicin in the co-cultured 01010627 GBM cells.

Temozolomide downregulates the Wnt3/GSK3/β-catenin/ABCB1 axis and increases the efficacy of doxorubicin in co-cultures of human primary BBB cells and glioblastoma cells.

We then asked the question whether the effects of TMZ could occur also in primary cells extracted from human brain microvessels, i.e. HMBECs.

We found that the promoter of *Wnt3* was fully unmethylated in HBMECs and that TMZ induced the partial methylation of the promoter (Figure 7a). This was followed by the decrease of Wnt3 mRNA (Figure 7b) and protein (Figure 7c), the increase of phospho(Tyr216)GSK3 and phospho(Ser33/37-Thr41)β-catenin (Figure 7c), the reduction of the β-catenin binding on *mdr1* promoter (Figure 7d), the decrease of Pgp/ABCB1 protein (Figure 7e). In co-cultures of HBMECs and primary GBM 01010627 cells, the intratumor delivery of doxorubicin was low (Figure 7f). Neither doxorubicin or TMZ induced significant cytotoxicity, measured in terms of extracellular release of LDH and activation of the caspase 3, in GBM cells co-cultured with HBMECs (Figure 7g). By contrast, the addition of TMZ on the luminal side of HBMECs, at a concentration that did not induce cytotoxicity (Online Resource 11a) and did not reduce the proliferation (Online Resource 11b) of endothelial cells, significantly increased the delivery of doxorubicin and cytotoxicity in GBM cells (Figure 7f-g).

Discussion

While the effect of TMZ on GBM cells is well known, no studies have investigated yet the effects of the drug on BBB cells. To explore this issue, we exposed human immortalized brain microvascular endothelial cells hCMEC/D3 and primary brain microvascular endothelial cells HBMECs to TMZ, at a concentration found in the blood of patients [30]. At this concentration the drug did not induce any detectable cytotoxic effect on BBB cells, but was able to increase the permeability of substrates of Pgp/ABCB1 across the BBB monolayer. Unlike other permeabilizing strategies [9, 10], TMZ

did not affect the integrity of tight junctions, as the permeability to dextran, inulin and sucrose, as well as the expression of claudin-5, occludin and ZO-1 did not change. Only claudin-3 was slightly reduced by TMZ: since Wnt3/β-catenin has been reported to up-regulate claudin-3 in mouse brain microvascular endothelial cells [35], this effect may be caused by the decrease in Wnt3 signalling induced by TMZ. However, as it appears from the permeability assay, the isolated decrease of claudin-3 was not sufficient enough for the functional impair of the tight junctions in hCMEC/D3 cells.

The reduction of Pgp/ABCB1 caused the increase in the permeability of doxorubicin and vinblastine elicited by TMZ. To the best of our knowledge, this effect of TMZ was not described before. This observation may have a strong impact on what we know about drug delivery to CNS, as Pgp/ABCB1 is abundantly localized on the luminal side of BBB cells [37] and recognizes a broad spectrum of substrates. Among these substrates, more specifically, is the majority of anticancer drugs [8], prevented from reaching therapeutic concentrations in CNS via this mechanism. The half-life of TMZ in plasma is short and the drug is chemically converted into its active metabolite MTIC [3]; it is conceivable that such a chemical conversion occurs also in our experimental system and that MTIC is the actual responsible for the effects on BBB cells.

The effect of TMZ was specific for Pgp/ABCB1, since the activity and expression of MRP1/ABCC1 and BCRP/ABCG2, two other ABC transporters present on BBB cells [8, 11, 37], were not affected. The decrease of Pgp/ABCB1 without changes in other ABC transporters is of particular interest. Indeed mice knocked down for Pgp/ABCB1 have a compensatory increase of BCRP/ABCG2 in BBB, suggesting a cooperation between these transporters [11]. Our study was performed by treating cells with a single dose of TMZ for 72 h; we did not investigate whether different experimental conditions (e.g. repetitive treatments with the drug or longer treatment periods) affect the expression of ABC transporters other than Pgp/ABCB1. The antitumor effects of TMZ, in terms of alkylating efficacy and DNA damages, are significantly stronger when the drug is administered repetitively within the same day than when the drug is administered as single dose [4]. We cannot exclude *a priori* that prolonged or repetitive administrations of TMZ might exert a stronger decrease in Pgp/ABCB1, thereby triggering a progressive increase in BCRP/ABCG2. When BCRP/ABCG2 is increased in response to the decrease of Pgp/ABCB1, drugs that are dual substrates of these transporters are not more delivered through the BBB [11]. Notwithstanding, the down-regulation of Pgp/ABCB1 results in the increased delivery of drugs, which have higher affinity for Pgp/ABCB1 than for BCRP/ABCG2 [11]. This is the case of doxorubicin and vinblastine, which are more transported across hCMEC/D3 monolayer upon the down-regulation of Pgp/ABCB1 induced by TMZ.

It has been reported that Pgp/ABCB1 is under the transcriptional control of β-catenin, whose activity is regulated by Wnt/GSK3/β-catenin axis in hCMEC/D3 cells [17, 18]. In our hands, untreated hCMEC/D3 cells had β-catenin constitutively bound on the promoter of *mdr1* gene and Pgp/ABCB1 constitutively expressed. In contrast, cells treated with

TMZ showed increased activity of GSK3 and increased amounts of phosphorylated β-catenin. The phosphorylation-dependent degradation of β-catenin resulted in a decrease of its nuclear translocation and binding on the *mdr1* promoter. The results with activators and inhibitors of the Wnt canonical pathway suggested that TMZ down-regulated Pgp/ABCB1 acting like a Wnt-pathway inhibitor. Of note, the same effect of Wnt/GSK3/β-catenin axis in controlling the expression of Pgp/ABCB1 and the same effect of TMZ occurred in primary HBMECs. Unlike previous observations, that showed that the inhibitor of GSK3 6-bromoindirubin-3'-oxime up-regulated the transcription of MRP2/ABCC2, MRP4/ABCC4 and BCRP/ABCG2, and the inhibitor of β-catenin quercetin produced the opposite effects [17], we did not find any change in the expression of BCRP/ABCG2 in hCMEC/D3 cells after TMZ. This discrepancy could owe to the different stimuli used. Quercetin inhibited the binding of TCF to its DNA target sequences [38], therein reducing the transcriptional activity of β-catenin/TCF complex. TCF is paramount in the activation of certain promoters, less so in the activation of others. We hypothesized that the transcription of *bcrp* gene may be tightly dependent on the whole β-catenin/TCF complex, whereas the transcription of *mdr1* gene may be less so. Although we did not measure the amount of TCF in hCMEC/D3 cells treated with TMZ and we cannot exclude that the drug may also interfere with the formation of the β-catenin/TCF complex, our data strongly suggest that TMZ down-regulated β-catenin at an upstream level, by preventing its nuclear translocation and the subsequent association with TCF. Alternatively, we may speculate that the down-regulation of *bcrp* gene due to the lower activation of β-catenin is masked by the simultaneous compensatory up-regulation of *bcrp,* consequent to the decrease of Pgp/ABCB1 [11]. The sum of these two events may leave unchanged the levels of BCRP/ABCG2 protein in cells treated with TMZ.

Our results are in agreement with other reports showing that Wnt signalling is involved in the Pgp-mediated chemoresistance in tumors. The Frizzled-1 receptor of Wnt, necessary for the activation of β-catenin pathway, is present at high levels in neuroblastoma [19] and breast cancers [39] overexpressing Pgp/ABCB1, where the silencing of Frizzled-1 down-regulated the *mdr1* gene. However, we did not detect any change in the expression levels of Frizzled in hCMEC/D3 cells exposed to TMZ. We therefore moved our focus on the levels of Wnt ligands produced by endothelial cells, which are able to bind Frizzled receptors and activate the GSK3/β-catenin axis. Wnt3 was present in both hCMEC/D3 and HBMEC cells; the results in Wnt3-silenced hCMEC/D3 cells supported the hypothesis that Wnt3 was a critical controller of *mdr1* transcription, since its depletion produced a 70% decrease in Pgp/ABC1 protein.

Interestingly, TMZ decreased Wnt3 protein and mRNA, leading us to hypothesize that the drug down-regulated the transcription of Wnt3 gene in BBB cells. As an alkylating agent, TMZ methylates guanine on O^6 position and induces a DNA mismatch repair response that produces double strand breaks, if not repaired by the O^6methylguanine

methyltransferase enzyme. However, the vast majority of the methylations caused by TMZ are other methylations, usually not cytotoxic [4]. The consequences of these non toxic methylations have not been investigated yet. We found that TMZ methylates the promoter of *Wnt3* gene, which is rich of CpG islands. Untreated hCMEC/D3 and HBMEC cells express a fully unmethylated promoter, which is consistent with the constitutive transcription of Wnt3: the promoter's methylation induced by TMZ may explain the decrease of Wnt3, suggesting that TMZ is an epigenetic down-regulator of *Wnt3* gene. Of note, TMZ administered on the luminal side of hCMEC/D3 cells also decreased the *mdr1* levels in GBM cells growing under hCMEC/D3 monolayer: this means that the drug crossed – as expected – the BBB, and acted on both endothelial and tumor cells, increasing at the same time the permeability of BBB cells and the chemosensitivity of GBM cells. Experimental findings obtained in our laboratory suggest that TMZ down-regulates Pgp/ABCB1 in GBM cells with a Wnt3a-dependent mechanism (Riganti, unpublished data).

In view of our results, we think that clinically achievable doses of TMZ may facilitate the subsequent passage of anticancer drugs, not commonly used in the therapy of GBM because they are rapidly effluxed through the BBB by Pgp/ABCB1. Using doxorubicin as a prototype, we indeed observed in co-culture models of hCMEC/D3 or HBMEC with GBM cells that the pre-treatment of BBB cells with TMZ significantly increased the delivery of doxorubicin, induced marked cytotoxicity and reduced the proliferation of GBM cells. The increased permeability of doxorubicin induced by TMZ was likely triggered by the down-regulation of the Wnt3/GSK3/β-catenin/Pgp axis in BBB cells, since the same effect was achieved by depleting Wnt3 in hCMEC/D3 cells.

Several strategies that increase the delivery of doxorubicin to GBMs, such as encapsulating the drug in pegylated liposomes [7, 40] or loading it in BBB-targeting nanoparticles [41, 42], are under intensive investigations. Our approach is different as we studied a drug already commonly used in GBM therapy, like TMZ. The pharmacokinetics, the pharmacodynamic effects and the side-effects of TMZ and doxorubicin are well known. The combination of TMZ and doxorubicin is new and requires appropriate studies of pharmacokinetics and safety pharmacology. The results of the present study are paving the way to other studies on the antitumor efficacy of this new drug combination in orthotopic animal models of human glioblastoma.

The same chemosensitizing effects of TMZ that we describe here were obtained with two other substrates of Pgp/ABCB1, vinblastine and topotecan. While the former is not currently used in GBM therapy, the latter has received a great deal of interest in the last few years. Although topotecan does not cross the BBB [6], it has a very low IC_{50} against GBM cells *in vitro* [27, 43] and has been proposed as an effective agent when administered by convection-enhanced delivery [6]. If the results obtained in our co-culture models will be confirmed *in vivo*, this might open the door for new therapeutic protocols

based on the pre-treatment with TMZ followed by systemic administration of topotecan. Our findings may also explain the clinical observation that the topoisomerase I inhibitors produce significant benefits in patients with recurrent gliomas when used in combination with TMZ [5].

In conclusion, we describe a novel role of TMZ in BBB cells, as a down-regulator of the expression of Pgp/ABCB1 at clinically achievable concentrations. Beside opening the door for new treatment protocols, our results might have important implications for the eradication of GBM cells in the BAT area, where tumor cells lay surrounded by intact BBB [8], cannot be completely removed by surgery or efficiently radiated and almost never are reached by effective concentrations of chemotherapeutic drugs. The use of TMZ in association with doxorubicin, topotecan or vinblastine may become a successful strategy for eradicating GBM cells from BAT area and preventing recurrence.

Acknowledgments.
We are indebted with Prof. Michele Lanotte (Department of Neuroscience, Neurosurgical Unit, University of Turin) and with Dr. Rossella Galli (San Raffaele Scientific Institute, Milan) for providing the primary glioblastoma samples. We are grateful to Costanzo Costamagna (Department of Oncology, University of Turin) for the technical assistance and to Dr. Oriana Monzeglio (Neuro-bio-oncology Center, Policlinico di Monza Foundation) for the technical suggestions with methylation promoter assay.
This work has been supported by grants from Compagnia di San Paolo, Italy (Neuroscience Program; grant 2008.1136) and Italian Association for Cancer Research (AIRC; MFAG 11475) to Chiara Riganti.
Martha Leonor Pinzón-Daza is recipient of a ERACOL Erasmus Mundus fellowship. Joanna Kopecka is recipient of a "Mario and Valeria Rindi" fellowship provided by Italian Foundation for Cancer Research (FIRC).

Conflict of interests.

None.

References

1. Bai RY, Staedke V, Riggins GJ (2011) Molecular targeting of GBM: Drug discovery and therapies. Trends Mol Med 17:301-332
2. Serwer LP, James CD (2012) Challenges in drug delivery to tumors of the central nervous system: An overview of pharmacological and surgical considerations. Adv Drug Deliv Rev 64:590-597
3. Saleem A, Brown GD, Brady F, Aboagye EO, Osman S, Luthra SK, Ranicar AS, Brock CS, Stevens MF, Newlands E, Jones T, Price P (2003) Metabolic activation of temozolomide measured in vivo using positron emission tomography. Cancer Res 63:2409-2415
4. Wick W, Plattan M, Weller M (2009) New (alternative) temozolomide regimens fort he treatment of glioma. Neuro Oncol 11:69-79
5. Vredenburgh JJ, Desjardins A, Reardon DA, Peters KB, Herndon JE 2nd, Marcello J, Kirkpatrick JP, Sampson JH, Bailey L, Threatt S, Friedman AH, Bigner DD, Friedman HS (2011) The addition of bevacizumab to standard radiation therapy and temozolomide followed by bevacizumab, temozolomide, and irinotecan for newly diagnosed glioblastoma. Clin Cancer Res 17:4119-4124

6. Lopez KA, Tannenbaum AM, Assanah MC, Linskey K, Yun J, Kangarlu A, Gil OD, Canoli P, Bruce JN (2011) Convection-enhanced delivery of topotecan into PDGF-driven model of glioblastoma prolongs survival and ablates both tumor-initiating cells recruited glial progenitors. Cancer Res 71:3963-3971
7. Hau P, Fabel K, Baumgart U, Rummele P, Grauer O, Bock A, Dietmaier C, Dietmaier W, Dietrich J, Dudel C, Hubner F, Jaucj T, Drechsel E, Kleiter I, Wismeth C, Zellner A, Brawanski A, Steinbrecher A, Marienhagen J, Bogdahan U (2004). Pegylated liposomal doxorubicin-efficacy in patients with recurrent high-grade glioma. Cancer 100:1199-1207
8. Agarwal S, Sane R, Oberoi R, Ohlfest JR, Elmquist WF (2011). Delivery of molecularly targeted therapy to malignant glioma, a disease of the whole brain. Expert Rev Mol Med 13:e17
9. Guillaume DJ, Doolittle ND, Gahramanov S, Hedrick NA, Delashaw JB, Neuwelt EA (2010) Intra-arterial chemotherapy with osmotic blood-brain barrier disruption for aggressive oligodendroglial tumors: results of a phase I study. Neurosurgery 66:48-58
10. Liu H-L, Hua M-Y, Chen P-Y, Chu P-C, Pan C-H, Yang H-W, Wuang C-Y, Wang J-J, Yen T-C, Wei K-C (2010) Blood-brain barrier disruption with focused ultrasound enhanced delivery of chemotherapeutic drugs for glioblastoma treatment. Radiology 255:415-425
11. Agarwal S, Hartz AM, Elmquist WF, Bauer B (2011) Breast cancer resistance protein and P-glycoprotein in brain cancer: two gatekeepers team up. Curr Pharm Des 17:2793-2802
12. Poller B, Drewe J, Krähenbühl S, Huwyler J, Gutmann H (2010) Regulation of BCRP (ABCG2) and P-glycoprotein (ABCB1) by cytokines in a model of the human blood-brain barrier. Cell Mol Neurobiol 30:63-70
13. Chan GNY, Hoque MT, Cummins CL, Bendayan R (2011) Regulation of P-glycoprotein by orphan nuclear receptors in human brain microvessel endothelial cells. J Neurochem 118:163-175
14. Wang X, Hawkins BT, Miller DS (2011). Aryl hydrocarbon receptor-mediated up-regulation of ATP-driven xenobiotic efflux transporters at the blood-brain barrier. FASEB J 25:644-652
15. Daneman R, Agalliu D, Zhoy L, Kuhnert F, Kuo CJ, Barres BA (2009) Wnt/β-catenin signalling is required for CNS, but not non-CNS, angiogenesis. Proc Natl Acad Sci USA 106:641-646
16. Liebner S, Plate KH (2010) Differentiation of the brain vasculature: the answer came blowing by the Wnt. J Angiogen Res 2:1-10
17. Lim JC, Kania KD, Wijesuriya H, Chawla S, Sethi JK, Pulaski L, Romero IA, Couraud PO, Weksler BB, Hladky SB, Barrand MA (2008) Activation of β-catenin signalling by GSK-3 inhibition increases p-glycoprotein expression in brain endothelial cells. J Neurochem 106:1855-1865
18. Kania KD, Wijesuriya HC, Hladky SB, Barrand MA (2011) Beta amyloid effects on expression of multidrug efflux transporters in brain endothelial cells. Brain Res 1418:1-11
19. Flahaut M, Meier R, Coulon A, Nardou KA, Niggli FK, Martinet D, Beckmann JS, Joseph J-M, Muhlethaler-Mottet A, Gross N (2009) The Wnt receptor FZD1 mediates chemoresistance in neuroblastoma through activation of the Wnt/b-catenin pathway. Oncogene 28:2245-2256
20. Schaich M, Kestel L, Pfirrmann M, Robel K, Illmer T, Kramer M, Dill C, Ehninger G, Schackert G, Krex D (2009) A MDR1 (ABCB1) gene single nucleotide polymorphism predicts outcome of temozolomide treatment in GBM patients. Annal Oncol 20:175-181
21. Weksler BB, Subileau EA, Perrière N, Charneau P, Holloway K, Leveque M, Tricoire-Leignel H, Nicotra A, Bourdoulous S, Turowski P, Male DK, Roux F, Greenwood J, Romero IA, Couraud PO (2005) Blood-brain barrier-specific properties of a human adult brain endothelial cell line. FASEB J 19:1872-1874
22. Monnaert V, Betbeder D, Fenart L, Bricout H, Lenfant AM, Landry C, Cecchelli R, Monflier E, Tilloy S (2004) Effects of γ- and hydroxypropyl- γ -cyclodextrins on the transport of doxorubicin across an in vitro model of blood-brain barrier. J Pharmacol Exp Ther 311:1115-1120
23. Siflinger-Birnboim A, Del Vecchio PJ, Cooper JA, Blumenstock FA, Shepard JM, Malik AB (1987) Molecular sieving characteristics of the cultured endothelial monolayer. J Cell Physiol 132:111-117
24. Campia I, Gazzano E, Pescarmona G, Ghigo D, Bosia A, Riganti C (2009) Digoxin and ouabain increase the synthesis of cholesterol in human liver cells. Cell Mol Life Sci 66:1580-1594
25. Broadley KW, Hunn MK, Farrand KJ, Price KM, Grasso C, Miller RJ, Hermans IF, McConnell MJ (2011) Side population is not necessary or sufficient for a cancer stem cell phenotype in glioblastoma multiforme. Stem Cells 29:452-461
26. Liu Y, Yang G, Bu X, Liu G, Ding J, Li P, Jia W (2011) Cell-type-specific regulation of raft-associated Akt signalling. Cell Death Dis 2:e145
27. Carcaboso AM, Elmeliegy MA, Shen J, Juel SJ, Zhang ZM, Calabrese C, Tracey L, Waters CM, Stewart CF (2010) Tyrosine kinase inhibitor gefitinib enhances topotecan penetration of gliomas. Cancer Res 70:4499-4508
28. Kopecka J, Campia I, Olivero P, Pescarmona G, Ghigo D, Bosia A, Riganti C (2011) A LDL-masked liposomal-doxorubicin reverses drug resistance in human cancer cells. J Contr Rel 149:196-205

29. Pinzón-Daza ML, Garzón R, Couraud PO, Romero IA, Weksler B, Ghigo D, Bosia A, Riganti C (2012) The association of statins plus LDL receptor-targeted liposome-encapsulated doxorubicin increases the in vitro drug delivery across blood-brain barrier cells. Brit J Pharmacol 167:1431-1447
30. Portnow J, Badie B, Chen M, Liu A, Blanchard S, Synold TW (2009) The neuropharmacokinetics of temozolomide in patients with resectable brain tumors: potential implications for the current approach to chemoradiation. Clin Cancer Res 15:7092-7098
31. Dalmark M, Storm HH (1981) A Fickian diffusion transport process with features of transport catalysis. Doxorubicin transport in human red blood cells. J Gen Physiol 78:349-364
32. Ito S, Woodland C, Sarkadi B, Hockmann G, Walker SE, Koren G (1999) Modeling of P-glycoprotein-involved epithelial drug transport in MDCK cells. Am J Physiol 277:F84-96
33. Goodwin AM, Sullivan KM, D'Amore PA (2006) Cultured Endothelial Cells Display Endogenous Activation of the Canonical Wnt Signalling Pathway and Express Multiple Ligands, Receptors, and Secreted Modulators of Wnt Signalling. Dev Dyn 235:3110-3120
34. Fu L, Zhang C, Zhang LY, Dong SS, Lu LH, Chen J, Dai Y, Li Y, Kong KL, Kwong DL, Guan XY (2011) Wnt2 secreted by tumor fibroblasts promotes tumor progression in oesophageal cancer by activation of the Wnt/β-catenin signalling pathway. Gut 60:1635-1643
35. Liebner S, Corada M, Bangsow T, Babbage J, Taddei A, Czupalla CJ, Reis M, Felici A, Wolburg H, Fruttiger M, Taketo MM, von Melchner H, Plate KH, Gerhardt H, Dejana E (2008) Wnt/beta-catenin signalling controls development of the blood-brain barrier. J Cell Biol 183:409-417
36. Bernardi H, Gay S, Fedon Y, Vernus B, Bonnieu A, Bacou F (2011) Wnt4 activates the canonical β-catenin pathway and regulates negatively myostatin: functional implication in myogenesis. Am J Physiol Cell Physiol 300:C1122-1138
37. Tai LM, Loughlin AJ, Male DK, Romero IA (2009) P-glycoprotein and breast cancer resistance protein restrict apical-to-basolateral permeability of human brain endothelium to amyloid-β. J Cereb Blood Flow Metab 29:1079-1083
38. Park CH, Chang JY, Hahn ER, Park S, Kim HK, Yang CH (2005) Quercetin, a potent inhibitor against beta-catenin/Tcf signalling in SW480 colon cancer cells. Biochem Biophys Res Commun 328:227-234
39. Zhang H, Zhang Z, Wu X, Li W, Su W, Su P, Cheng H, Xiang L, Gao P, Zhou G (2012) Interference of Frizzled 1 (FD1) reverses multidrug resistance in breast cancer cells through the Wnt/β-catenin pathway. Cancer Lett 323:106-113
40. Ananda S, Nowak AK, Cher L, Dowling A, Brown C, Simes J, Rosenthal MA and the Cooperative Trials Group for Neuro-Oncology (COGNO) (2011) Phase 2 trial of temozolomide and pegylated liposomal doxorubicin in the treatment of patients with glioblastoma multiforme following concurrent radiotherapy and chemotherapy. J Clin Neurosci 18:1444-1448
41. Steiniger SC, Kreuter J, Khalansky AS, Skidan IN, Bobruskin AI, Smirnova ZS, Severin SE, Uhl R, Kock M, Geiger KD, Gelperina SE (2004) Chemotherapy of glioblastoma in rats using doxorubicin-loaded nanoparticles. Int J Cancer 109:759-767
42. Wohlfart S, Khalansky AS, Gelperina S, Begley D, Kreuter J (2011) Kinetics of transport of doxorubicin bound to nanoparticles across the blood-brain barrier. J Control Rel 154:103-107
43. Yount G, Yang Y, Wong B, Wang H-J, Yang L-X (2007) A novel camptothecin analog with enhanced antitumor activity. Anticancer Res 27:3173-3178

Figure legends

Fig 1 Effects of temozolomide on permeability coefficients, tight junction markers and ABC transporters in blood-brain barrier hCMEC/D3 cells

a. hCMEC/D3 cells were grown for 7 days up to confluence in Transwell inserts, without (*CTRL*) or with temozolomide (*TMZ;* 50 μmol/L for the last 72 h). At the end of the incubation period, 2 μmol/L dextran-FITC, 2 μCi/mL [^{14}C]-inulin, 2 μCi/mL [^{14}C]-sucrose, 5 μmol/L doxorubicin, 2 μCi/mL [^{3}H]-vinblastine, 10 μmol/L mitoxantrone were added in the upper chamber. After 3 h the amount of the drug recovered from the lower chamber was measured fluorimetrically (for dextran-FITC, doxorubicin, mitoxantrone) or by liquid scintillation (for inulin, sucrose, vinblastine). Permeability coefficients were calculated as reported under Materials and Methods. Measurements were performed in duplicate and data are presented as means $\pm$ SD (n = 3). Vs *CTRL*: * $p < 0.02$. **b.** hCMEC/D3 cells were incubated without (*CTRL*) or with temozolomide (*TMZ*; 50 μmol/L for 72 h), then lysed and subjected to Western blot analysis for claudin-3, claudin-5, occludin, ZO-1. β-tubulin expression was used as control of equal protein loading. The figure is representative of 3 experiments with similar results. The band density ratio between each protein and β-tubulin was expressed as arbitrary units. **c.** hCMEC/D3 cells, treated as reported in **b**, were subjected to the Western blot analysis for Pgp/ABCB1, MRP1/ABCC1, BCRP/ABCG2. β-tubulin expression was used as control of equal protein loading. The figure is representative of 3 experiments with similar

results. The band density ratio between each protein and β-tubulin was expressed as arbitrary units. Vs *CTRL*: * $p < 0.05$.

Fig 2 Effects of temozolomide on *mdr1* expression and GSK3/β-catenin pathway in hCMEC/D3 cells
hCMEC/D3 cells were grown in fresh medium (*CTRL*) or in the presence of temozolomide (*TMZ*; 50 μmol/L for 48 h), then subjected to the following investigations. **a.** Total RNA was extracted and reverse-transcribed, the expression of *mdr1* gene was detected by qRT-PCR. The expression level in untreated cells was considered "1". Data are presented as means ± SD (n = 3). Vs *CTRL*: * $p < 0.002$. **b.** Chromatin immunoprecipitation of β-catenin on *mdr1* promoter (*pro*) in hCMEC/D3 cells. *gen*: PCR product from genomic DNA. *no Ab*: precipitated samples without anti-β-catenin antibody. *bl*: blank. The figure is representative of 3 experiments with similar results. **c.** Nuclear and cytosolic extracts were analyzed for the amount of β-catenin. The expression of β-tubulin and TBP was used as control of equal protein loading for cytosolic and nuclear samples respectively, and to verify the efficacy of the nucleus-cytosol separation. The band density ratio between each protein and β-tubulin/TBP was expressed as arbitrary units. Vs *CTRL*: * $p < 0.05$. The figure is representative of 3 experiments with similar results. **d.** Western blot analysis of phospho(Tyr216)GSK3, GSK3, phospho(Ser33/37/Thr41)β-catenin, β-catenin in whole cell lysates. β-tubulin expression was used as control of equal protein loading. The figure is representative of 3 experiments with similar results. The band density ratio between each protein and β-tubulin was expressed as arbitrary units. Vs *CTRL*: * $p < 0.02$.

Fig 3 Effects of temozolomide and Wnt modulators on *mdr1* expression in hCMEC/D3 cells
hCMEC/D3 cells were grown in fresh medium (*CTRL*) or with temozolomide (*TMZ*; 50 μmol/L for 48 h), Wnt activator 2-amino-4-(3,4-(methylenedioxy)benzylamino)-6-(3-methoxyphenyl)pyrimidine (*WntA*; 20 μmol/L for 24 h), Wnt inhibitor recombinant Dkk-1 protein (*DKK*; 1 μg/mL for 24 h), GSK3 inhibitor LiCl (*LiCl*; 10 mmol/L for 24 h). When co-incubated, WntA and LiCl were added to TMZ in the last 24 h. **a.** Western blot analysis of phospho(Tyr216)GSK3, GSK3, phospho(Ser33/37/Thr41)β-catenin, β-catenin in whole cell lysates. β-tubulin expression was used as control of equal protein loading. The figure is representative of 3 experiments with similar results. The band density ratio between each protein and β-tubulin was expressed as arbitrary units. Vs *CTRL*: * $p < 0.02$; vs *WntA* or *LiCl* alone: ° $p < 0.05$. **b.** Nuclear and cytosolic extracts were analyzed for the amount of β-catenin. The expression of β-tubulin and TBP was used as control of equal protein loading for cytosolic and nuclear samples respectively, and to verify the efficacy of the nucleus-cytosol separation. The band density ratio between each protein and β-tubulin/TBP was expressed as arbitrary units. Vs *CTRL*: * $p < 0.05$; vs *WntA* or *LiCl* alone: ° $p < 0.005$. The figure is representative of 3 experiments with similar results. **c.** Chromatin immunoprecipitation of β-catenin on *mdr1* promoter (*pro*) in hCMEC/D3 cells. *gen*: PCR product from genomic DNA. *no Ab*: precipitated samples without anti-β-catenin antibody. *bl*: blank. The figure is representative of 3 experiments with similar results. **d.** *mdr1* expression was detected in triplicate by qRT-PCR. Data are presented as means ± SD (n = 4). Vs *CTRL*: * $p < 0.02$; vs *WntA* or *LiCl*: ° $p < 0.05$. **e.** Western blot analysis of Pgp/ABCB1. β-Tubulin expression was used as control of equal protein loading. The figure is representative of 3 experiments with similar results. The band density ratio between each protein and β-tubulin was expressed as arbitrary units. Vs *CTRL*: * $p < 0.01$; vs *WntA* or *LiCl* alone: ° $p < 0.02$. **f.** Doxorubicin permeability. hCMEC/D3 cells were grown for 7 days up to confluence in Transwell inserts and treated as reported above. At the end of the incubation period, 5 μmol/L doxorubicin was added in the upper chamber. After 3 h the amount of the drug recovered from the lower chamber was measured fluorimetrically. Permeability coefficient was calculated as reported under Materials and Methods. Measurements were performed in duplicate and data are presented as means ± SD (n = 3). Vs *CTRL*: * $p < 0.001$; vs *WntA* or *LiCl* alone: ° $p < 0.005$.

Fig 4 Effects of temozolomide on Wnt3 synthesis in hCMEC/D3 cells
hCMEC/D3 cells were grown in the absence (*CTRL*) or in the presence of temozolomide (*TMZ*; 50 μmol/L for 48 h in Western blot experiments, 24 h in qRT-PCR and MSP experiments), then subjected to the following investigations. **a.** Western blot analysis of Wnt3 in whole cell lysates. β-tubulin expression was used as control of equal protein loading. The figure is representative of 3 experiments with similar results. The band density ratio between Wnt3 and β-tubulin was expressed as arbitrary units. Vs *CTRL*: * $p < 0.05$. **b.** Total RNA was extracted and reverse-transcribed, then the expression of *Wnt3* gene was detected by qRT-PCR. The expression level in untreated cells was considered "1". Data are presented as means ± SD (n = 3). Vs *CTRL*: * $p < 0.05$. **c**. Methylation of *Wnt3* promoter. Genomic DNA was subjected to bisulfite modification, followed by PCR with specific primers for methylated (*M*) and unmethylated (*UM*) *Wnt3* promoter. The figure is representative of 3 experiments with similar results. +: positive controls with a universal methylated or unmethylated genome sequence, respectively. *bl*: blank.

Fig 5 Effects of Wnt3 silencing on *mdr1* expression in hCMEC/D3 cells

Wild-type hCMEC/D3 cells (*CTRL*), cells stably transfected with a non-targeting 29-mer scrambled shRNA (*scr*) or stably silenced for Wnt3 (*Wnt3*-) were subjected to the following investigations. **a.** Wnt3 qRT-PCR. Total RNA was extracted and reverse-transcribed, the expression of *Wnt3* gene was detected by qRT-PCR. The expression level in untreated cells was considered "1". Data are presented as means ± SD (n = 3). Vs *CTRL*: * $p < 0.001$. **b.** Western blot analysis of Wnt3 in whole cell lysates. Tubulin expression was used as control of equal protein loading. The figure is representative of 3 experiments with similar results. The band density ratio between Wnt3 and β-tubulin was expressed as arbitrary units. Vs *CTRL*: * $p < 0.001$. **c.** Western blot analysis of phospho(Tyr216)GSK3, GSK3, phospho(Ser33/37/Thr41)β-catenin, β-catenin in whole cell lysates. β-tubulin expression was used as control of equal protein loading. The figure is representative of 3 experiments with similar results. The band density ratio between each protein and β-tubulin was expressed as arbitrary units. Vs *CTRL*: * $p < 0.01$. **d.** Chromatin immunoprecipitation of β-catenin on *mdr1* promoter (*pro*) in hCMEC/D3 cells. *gen*: PCR product from genomic DNA. *no Ab*: precipitated samples without anti-β-catenin antibody. *bl*: blank. The figure is representative of 3 experiments with similar results. **e.** Western blot analysis of Pgp/ABCB1. β-tubulin expression was used as control of equal protein loading. The figure is representative of 3 experiments with similar results. The band density ratio between each protein and β-tubulin was expressed as arbitrary units. Vs *CTRL*: * $p < 0.002$. **f.** Doxorubicin permeability. hCMEC/D3 cells were grown for 7 days up to confluence in Transwell inserts, then 5 µmol/L doxorubicin was added in the upper chamber. After 3 h the amount of the drug recovered from the lower chamber was measured fluorimetrically. Permeability coefficient was calculated as reported under Materials and Methods. Measurements were performed in duplicate and data are presented as means ± SD (n = 3). Vs *CTRL*: * $p < 0.001$.

Fig 6 Effects of temozolomide on doxorubicin delivery and cytotoxicity in glioblastoma cells co-cultured with hCMEC/D3 cells

hCMEC/D3 cells were grown for 7 days up to confluence in Transwell inserts; CV17, 01010627 and U87-MG cells were seeded at day 4 in the lower chamber. After 3 days of co-culture, supernatant in the upper chamber was replaced with fresh medium without (-) or with temozolomide (50 µmol/L for 72 h; *TMZ* or *T*). 5 µmol/L doxorubicin (*dox*) was added in the upper chamber in the last 24 h, then the following investigations were performed. **a**. Fluorimetric quantification of intracellular doxorubicin in GBM cells. Measurements were performed in duplicate and data are presented as means ± SD (n = 4). Vs untreated cells: * $p < 0.05$. **b**. 01010627 cells were seeded on sterile glass coverslips, treated as reported above, then stained with DAPI and analyzed by fluorescence microscopy to detect the intracellular accumulation of doxorubicin. Magnification: 63 x objective (1.4 numerical aperture); 10 x ocular lens. The micrographs are representative of 3 experiments with similar results. **c**. The culture supernatant of GBM cells was checked spectrophotometrically for the extracellular activity of LDH (open bars), the cell lysates were analyzed fluorimetrically for the activity of caspase 3 (hatched bars). Measurements were performed in duplicate and data are presented as means ± SD (n= 4). Vs untreated cells: * $p < 0.05$. **d**. After 3 days of co-culture, the medium of the upper chamber was replaced with fresh medium (*open circles*) or medium containing 50 µmol/L temozolomide for 72 h (*solid circles*, *T*), 5 µmol/L doxorubicin for 24 h (*open squares*, *dox*), 50 µmol/L temozolomide for 72 h plus 5 µmol/L doxorubicin in the last 24 h (*solid squares*, *T* + *dox*). Drug treatments were repeated every 7 days, as reported in the Materials and methods section. The proliferation of GBM cells was monitored weekly by crystal violet staining. Measurements were performed in triplicate and data are presented as means ± SD (n= 4). Vs untreated cells (*CTRL*): * $p < 0.01$. *T* + *dox* vs *T* alone: ° $p < 0.05$. **e-f**. Wild-type hCMEC/D3 cells (*CTRL*), cells stably transfected with a non-targeting 29-mer scrambled shRNA (*scr*) or stably silenced for Wnt3 (*Wnt3*-) were grown for 7 days up to confluence in Transwell inserts; 01010627 GBM cells were seeded at day 4 in the lower chamber. After 3 days of co-culture, supernatant in the upper chamber was replaced with fresh medium without (- *dox*) or with 5 µmol/L doxorubicin (+ *dox*) for 24 h. The intracellular doxorubicin in GBM cells was measured fluorimetrically (panel **e**). Measurements were performed in duplicate and data are presented as means ± SD (n = 3). Vs untreated cells: * $p < 0.001$. The culture supernatant of GBM cells was checked spectrophotometrically for the extracellular activity of LDH (open bars, panel **f**), the cell lysates were analyzed fluorimetrically for the activity of caspase 3 (hatched bars, panel **f**). Measurements were performed in duplicate and data are presented as means ± SD (n= 3). Vs untreated cells: * $p < 0.001$.

Fig 7 Effects of temozolomide in primary human brain microvascular endothelial cells co-cultured with primary human glioblastoma cells

a. Methylation of *Wnt3* promoter. HBMECs were grown in the absence (*CTRL*) or in the presence of temozolomide (*TMZ*; 50 µmol/L, for 24 h), then genomic DNA was subjected to bisulfite modification, followed by PCR with specific primers for methylated (*M*) and unmethylated (*UM*) *Wnt3* promoter. The figure is representative of 3 experiments with similar results. +: positive controls with a universal methylated or unmethylated genome sequence, respectively. *bl*: blank. **b**. *Wnt3* mRNA levels. Cells were incubated in the absence (*CTRL*) or in the presence of temozolomide (*TMZ*; 50 µmol/L, for 48 h). Total RNA was extracted and reverse-transcribed, the expression of *Wnt3* gene was detected by qRT-PCR. The expression level in untreated cells was considered "1". Data are presented as means ± SD (n = 3). Vs *CTRL*: * $p < 0.02$. **c.** Western blot

analysis of Wnt3-signalling. Cells were incubated as reported in **b**, then lysed and subjected to the Western blot analysis of Wnt3, phospho(Tyr216)GSK3, GSK3, phospho(Ser33/37/Thr41)β-catenin, β-catenin in whole cell lysates. β-tubulin expression was used as control of equal protein loading. The figure is representative of 3 experiments with similar results. The band density ratio between each protein and β-tubulin was expressed as arbitrary units. Vs *CTRL*: * $p < 0.05$. **d**. Chromatin immunoprecipitation of β-catenin on *mdr1* promoter (*pro*) in cells incubated as reported in **b**. *gen*: PCR product from genomic DNA. *no Ab*: precipitated samples without anti-β-catenin antibody. *bl*: blank. The figure is representative of 3 experiments with similar results. **e**. Cells were incubated for 72 h without (*CTRL*) or with temozolomide (*TMZ*; 50 μmol/L), then lysed and subjected to Western blot analysis for Pgp/ABCB1. β-tubulin expression was used as control of equal protein loading. The figure is representative of 3 experiments with similar results. The band density ratio between each protein and β-tubulin was expressed as arbitrary units. Vs *CTRL*: * $p < 0.01$. **f.** HBMECs were grown for 7 days up to confluence in Transwell inserts; 01010627 GBM cells were seeded at day 4 in the lower chamber. After 3 days of co-culture, supernatant in the upper chamber was replaced with fresh medium without (*CTRL*) or with temozolomide (50 μmol/L for 72 h; *TMZ*). 5 μmol/L doxorubicin (*dox*) was added in the upper chamber in the last 24 h. GBM cells were then collected and analyzed for the intracellular amount of doxorubicin by a fluorimetric assay. Measurements were performed in duplicate and data are presented as means $\pm$ SD (n = 3). Vs untreated cells (*CTRL*): * $p < 0.001$. **g.** Co-cultures of HBMECs and 01010627 cells were set up as detailed in **f**. At the end of the incubation period, the culture supernatant of GBM cells was checked spectrophotometrically for the extracellular activity of LDH (open bars), the cell lysates were analyzed fluorimetrically for the activity of caspase 3 (hatched bars). Measurements were performed in duplicate and data are presented as means $\pm$ SD (n= 3). Vs untreated cells: * $p < 0.005$.

Fig 1

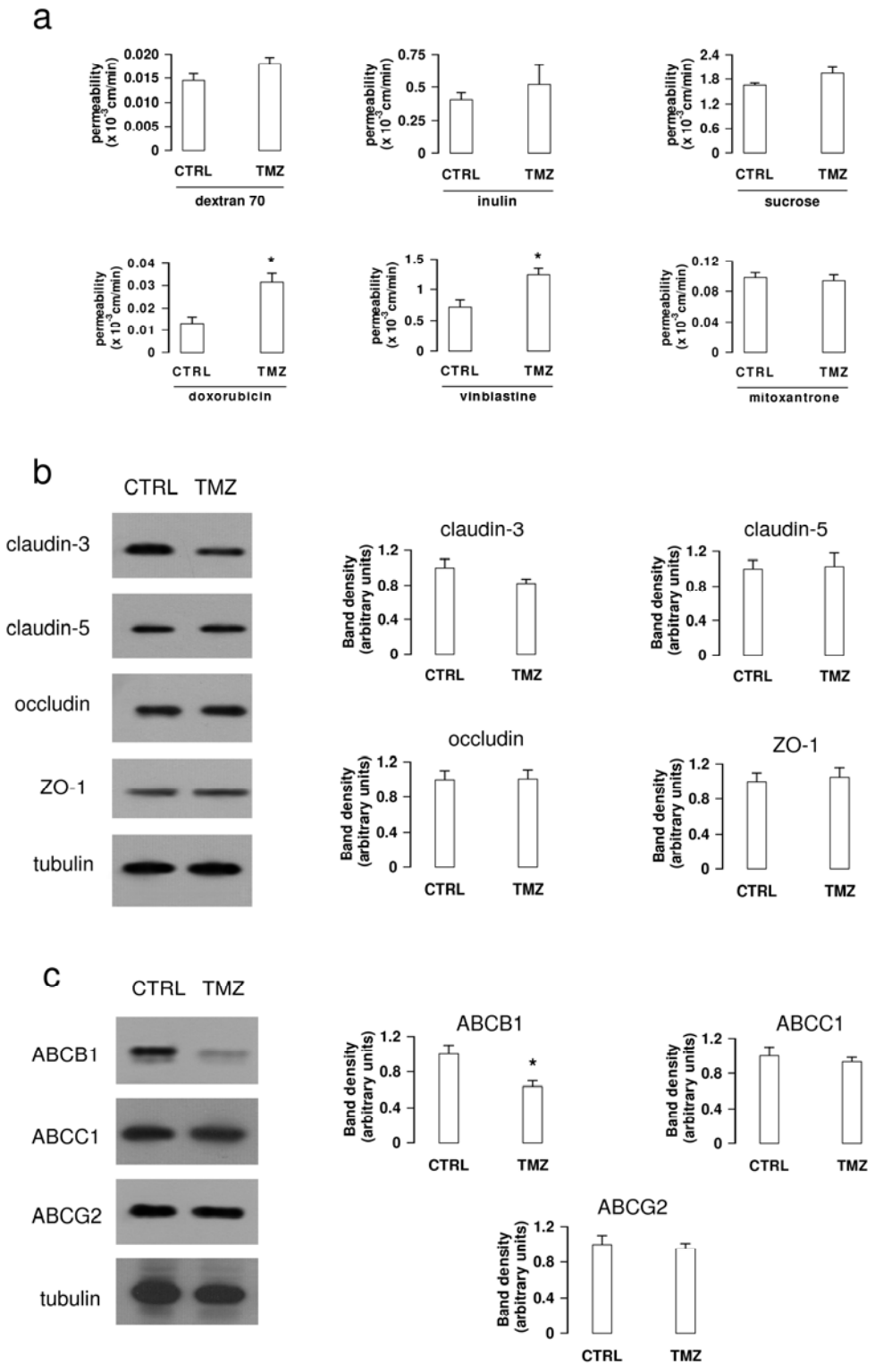
a
permeability (x 10-3 cm/min)
CTRL
TMZ
dextran 70
inulin
sucrose
doxorubicin
vinblastine
mitoxantrone
b
CTRL TMZ
claudin-3
claudin-5
occludin
ZO-1
tubulin
Band density (arbitrary units)
c
ABCB1
ABCC1
ABCG2

Fig 2

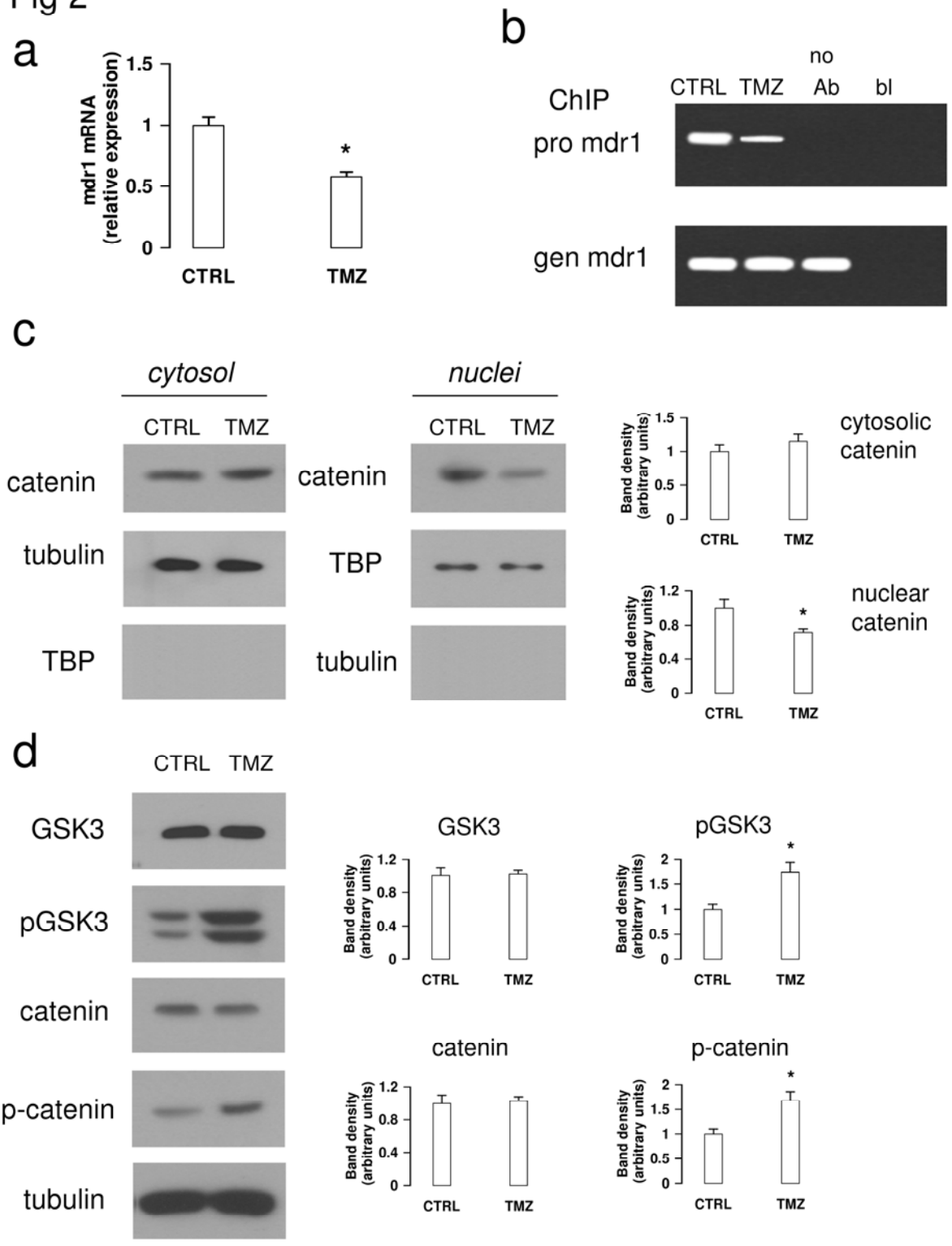
a
mdr1 mRNA (relative expression)
1.5
1
0.5
0
*
CTRL
TMZ
b
ChIP
no
CTRL TMZ Ab bl
pro mdr1
gen mdr1
c
cytosol
nuclei
CTRL TMZ
CTRL TMZ
catenin
tubulin
TBP
catenin
TBP
tubulin
Band density (arbitrary units)
cytosolic catenin
nuclear catenin
d
CTRL TMZ
GSK3
pGSK3
catenin
p-catenin
tubulin
GSK3
pGSK3
catenin
p-catenin

Fig 3

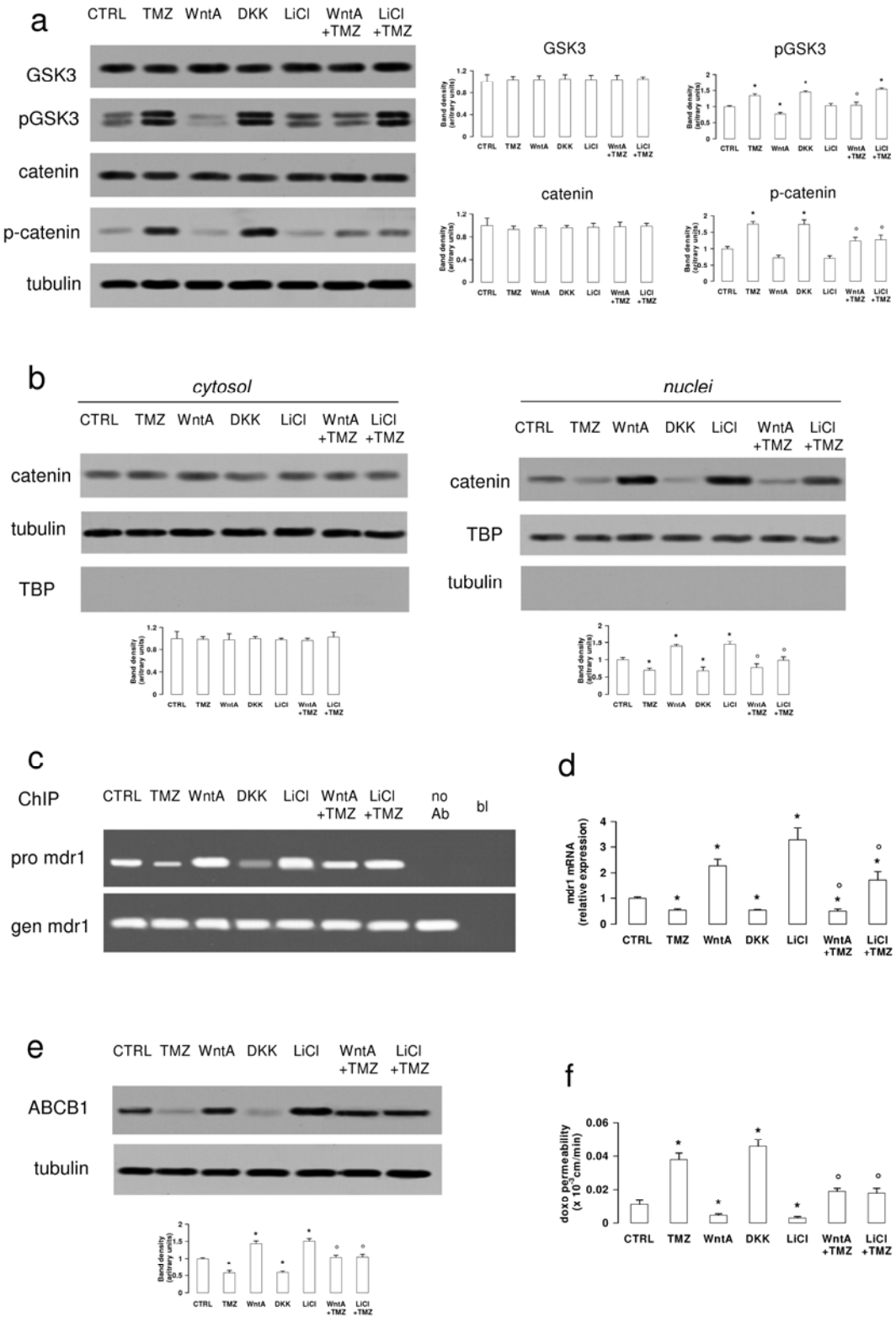
a
CTRL TMZ WntA DKK LiCl WntA +TMZ LiCl +TMZ
GSK3
pGSK3
catenin
p-catenin
tubulin
GSK3
pGSK3
catenin
p-catenin
b
cytosol
nuclei
CTRL TMZ WntA DKK LiCl WntA +TMZ LiCl +TMZ
catenin
tubulin
TBP
c
ChIP
CTRL TMZ WntA DKK LiCl WntA +TMZ LiCl +TMZ no Ab bl
pro mdr1
gen mdr1
d
mdr1 mRNA (relative expression)
CTRL TMZ WntA DKK LiCl WntA +TMZ LiCl +TMZ
e
CTRL TMZ WntA DKK LiCl WntA +TMZ LiCl +TMZ
ABCB1
tubulin
f
doxo permeability (x 10-3 cm/min)
CTRL TMZ WntA DKK LiCl WntA +TMZ LiCl +TMZ

Fig 4

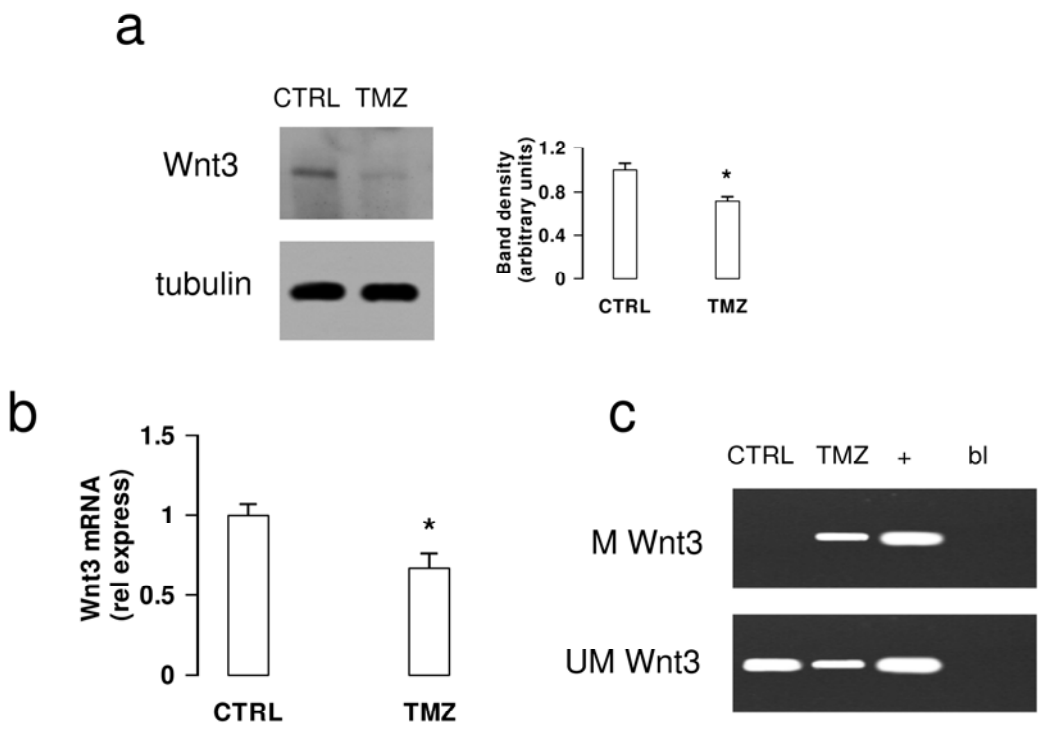
a
CTRL TMZ
Wnt3
tubulin
Band density (arbitrary units)
1.2
0.8
0.4
0
*
CTRL
TMZ
b
Wnt3 mRNA (rel express)
1.5
1
0.5
0
*
CTRL
TMZ
c
CTRL TMZ + bl
M Wnt3
UM Wnt3

Fig 5

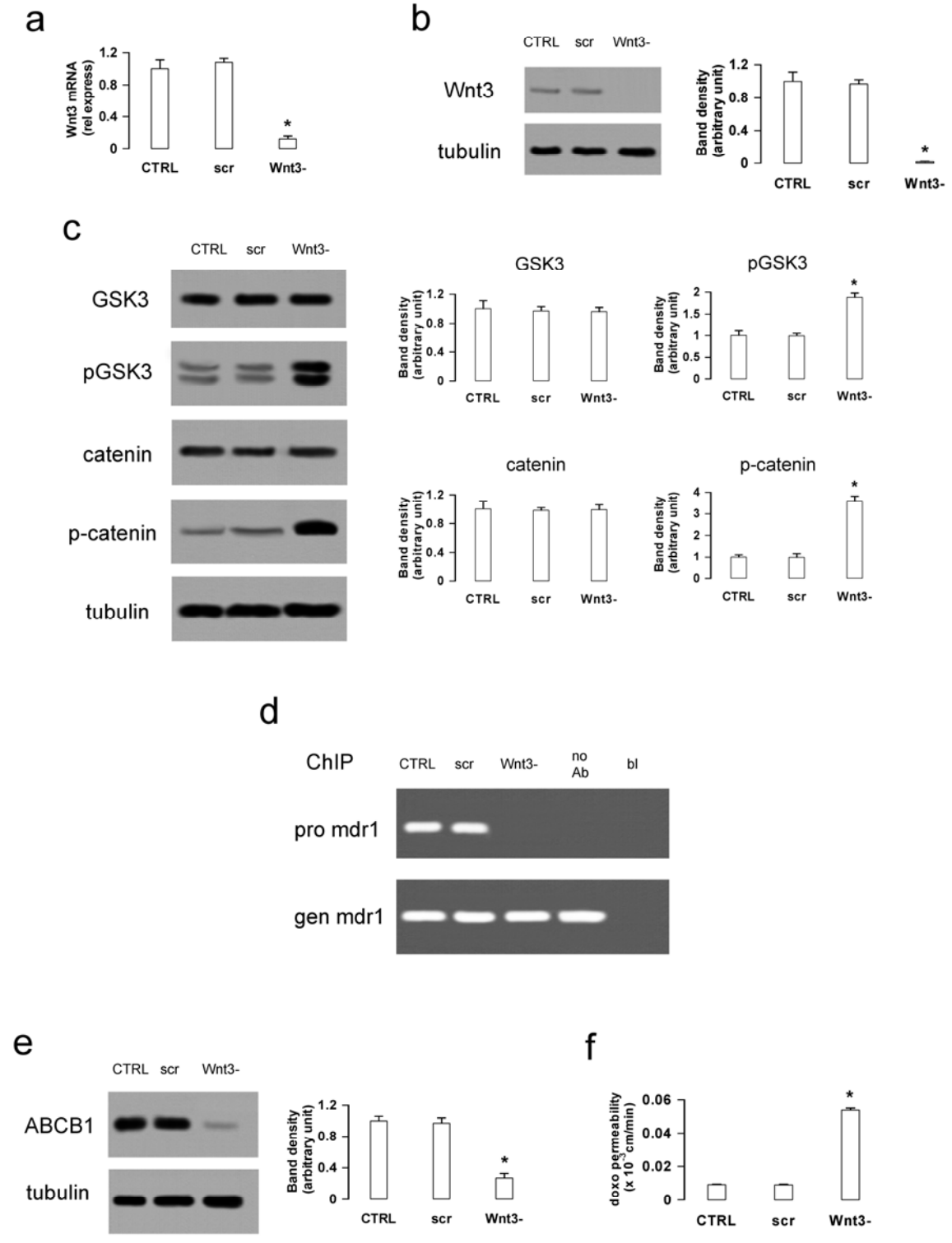
a
Wnt3 mRNA (rel express)
1.2
0.8
0.4
0
CTRL
scr
Wnt3-
b
CTRL scr Wnt3-
Wnt3
tubulin
Band density (arbitrary unit)
c
GSK3
pGSK3
catenin
p-catenin
tubulin
d
ChIP
CTRL scr Wnt3- no Ab bl
pro mdr1
gen mdr1
e
ABCB1
tubulin
f
doxo permeability (x 10⁻³ cm/min)
0.06
0.04
0.02

Fig 6

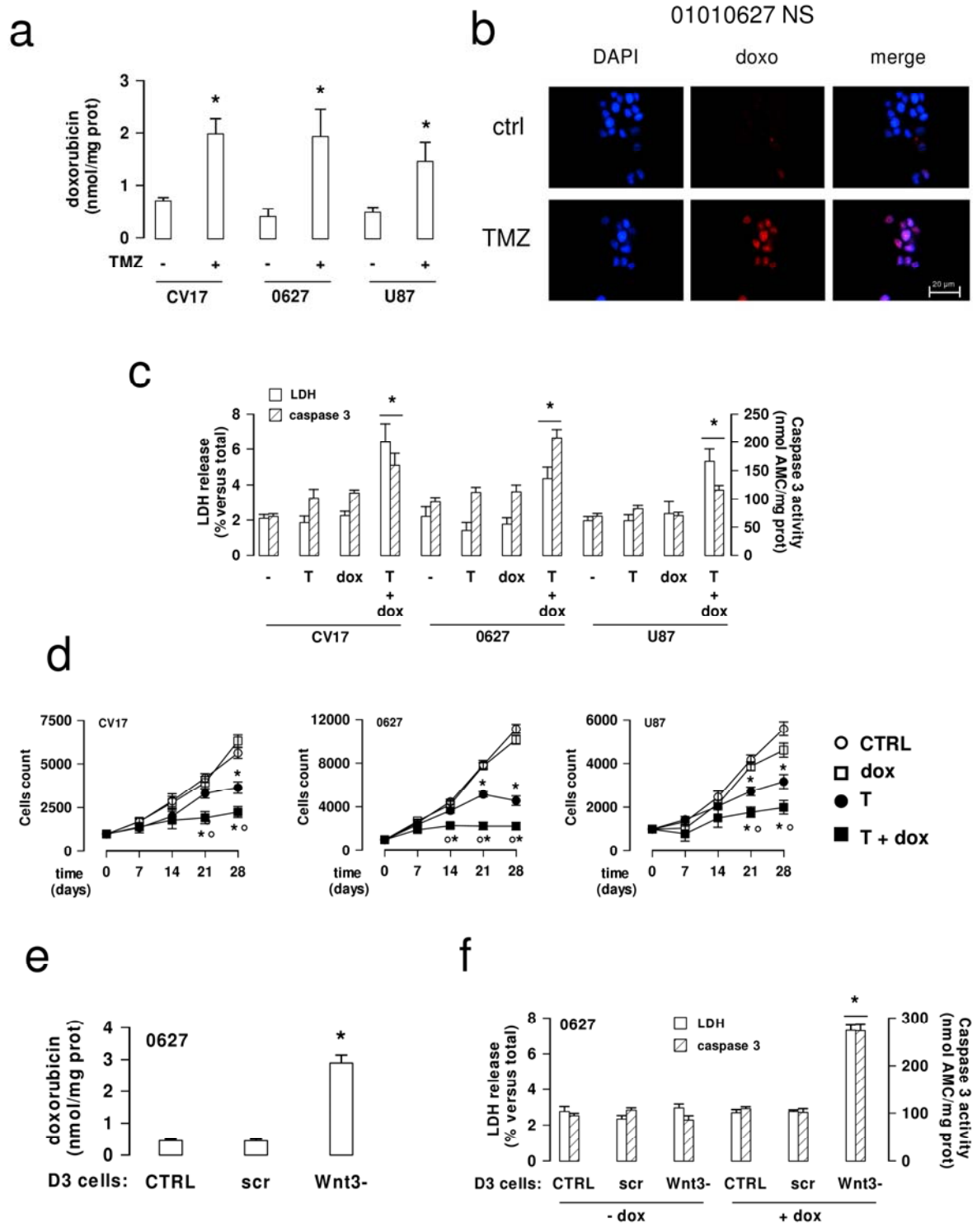
a
doxorubicin (nmol/mg prot)
TMZ
CV17
0627
U87
b
01010627 NS
DAPI
doxo
merge
ctrl
TMZ
c
LDH
caspase 3
LDH release (% versus total)
Caspase 3 activity (nmol AMC/mg prot)
CV17
0627
U87
d
CV17
0627
U87
Cells count
time (days)
CTRL
dox
T
T + dox
e
0627
doxorubicin (nmol/mg prot)
D3 cells: CTRL scr Wnt3-
f
0627
LDH
caspase 3
LDH release (% versus total)
Caspase 3 activity (nmol AMC/mg prot)
D3 cells: CTRL scr Wnt3- CTRL scr Wnt3-
- dox
+ dox

Fig 7

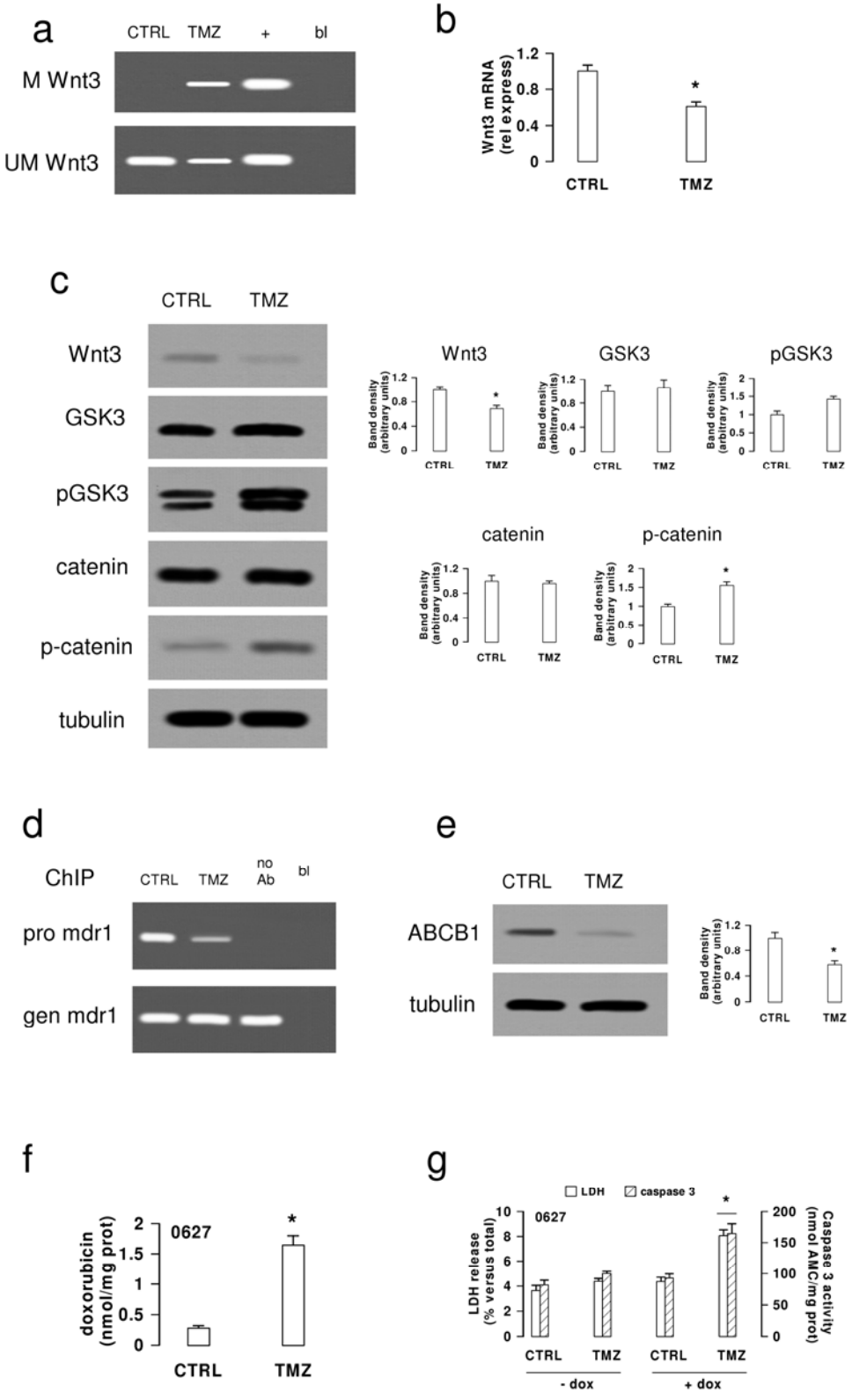
a
CTRL
TMZ
+
bl
M Wnt3
UM Wnt3
b
Wnt3 mRNA (rel express)
1.2
0.8
0.4
0
*
CTRL
TMZ
c
CTRL
TMZ
Wnt3
GSK3
pGSK3
catenin
p-catenin
tubulin
Wnt3
GSK3
pGSK3
catenin
p-catenin
Band density (arbitrary units)
CTRL
TMZ
d
ChIP
CTRL
TMZ
no Ab
bl
pro mdr1
gen mdr1
e
CTRL
TMZ
ABCB1
tubulin
Band density (arbitrary units)
f
doxorubicin (nmol/mg prot)
2
1.5
1
0.5
0
0627
*
CTRL
TMZ
g
LDH
caspase 3
LDH release (% versus total)
Caspase 3 activity (nmol AMC/mg prot)
0627
*
CTRL
TMZ
CTRL
TMZ
- dox
+ dox

Supplementary Material

Temozolomide down-regulates P-glycoprotein in human blood-brain barrier cells by disrupting Wnt3-signaling.

Chiara Riganti[1,2], Iris C. Salaroglio[1], Martha L. Pinzòn-Daza[1,3], Valentina Caldera[4], Ivana Campia[1], Joanna Kopecka[1], Marta Mellai[4], Laura Annovazzi[4], Pierre-Olivier Couraud[5], Amalia Bosia[1,2], Dario Ghigo[1,2], Davide Schiffer[4]

[1] *Department of Oncology, University of Turin, Via Santena, 5/bis, 10126, Turin, Italy*

[2] *Research Center on Experimental Medicine (CeRMS), University of Turin, Via Santena, 5/bis, 10126, Turin, Italy*

[3] *Unidad de Bioquímica, Facultad de Ciencias Naturales y Matemáticas, Universidad del Rosario, Carrera 6, Bogotá, Colombia*

[4] *Neuro-bio-oncology Center, Policlinico di Monza Foundation, Via Pietro Micca 29, 13100, Vercelli, Italy*

[5] *Institut Cochin, Centre National de la Recherche Scientifique UMR 8104, Institut National de la Santé et de la Recherche Médicale (INSERM) U567, Université René Descartes, 22 rue Méchain, 75014 Paris, France*

Corresponding author: Dr. Chiara Riganti, Department of Oncology, University of Turin, Via Santena 5/bis, 10126 Turin, Italy - Phone: +39-11-6705857; fax: +39-11-6705845; e-mail: chiara.riganti@unito.it

Online Resource 1

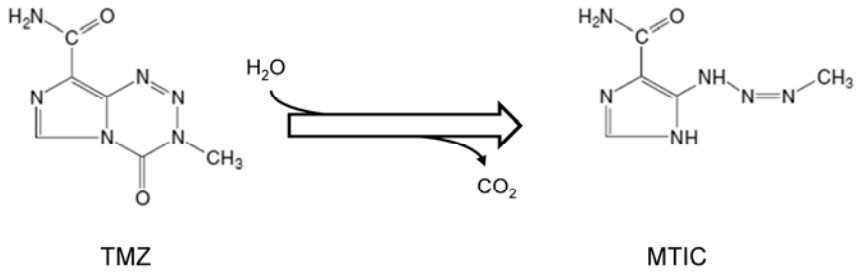

Online Resource 1. Chemical structure of temozolomide (TMZ) and its metabolite 3-methyl-(triazen-1-yl)imidazole-4-carboxamide (MTIC).

Online Resource 2

Primers sequences of quantitative Real Time-PCR (qRT-PCR), chromatin immunoprecipitation (ChIP) and methylation specific PCR (MSP).

Gene	Assay	Forward primer (5'-3')	Reverse primer (5'-3')
mdr1	qRT-PCR	TGCTGGAGCGGTTCTACG	ATAGGCAATGTTCTCAGCAATG
Wnt2b	qRT-PCR	GTGTCCTGGCTGGTTCCTTA	GAAGCTGGTGCAAAGGAAAG
Wnt3	qRT-PCR	ACGAGAACTCCCCCAACTTT	GATGCAGTGGCATTTTTCCT
Wnt4	qRT-PCR	GCTGTGACAGGACAGTGCAT	GCCTCATTGTTGTGGAGGTT
β-actin	qRT-PCR	GCTATCCAGGCTGTGCTATC	TGTCACGCACGATTTCC
mdr1 (promoter)	ChIP	CGATCCGCCTAAGAACAAAG	AGCACAAATTGAAGGAAGGAG
mdr1 (upstream sequence)	ChIP	GTGGTGCCTGAGGAAGAGAG	GCAACAAGTAGGCACAAGCA
mdr1 (genomic)	ChIP	GACCAAGCTCTCCTTGCATC	AGGGAAGTCTGGCAGCTGTA
Wnt3 promoter (methylated)	MSP	GAATTTTATTGAGGTTGTGGGTTAC	TTATCAAAAATCAAATCGATATCGA
Wnt3 promoter (unmethylated)	MSP	ATTTTATTGAGGTTGTGGGTTATGT	TATCAAAAATCAAATCAATATCAAA

Online Resource 3

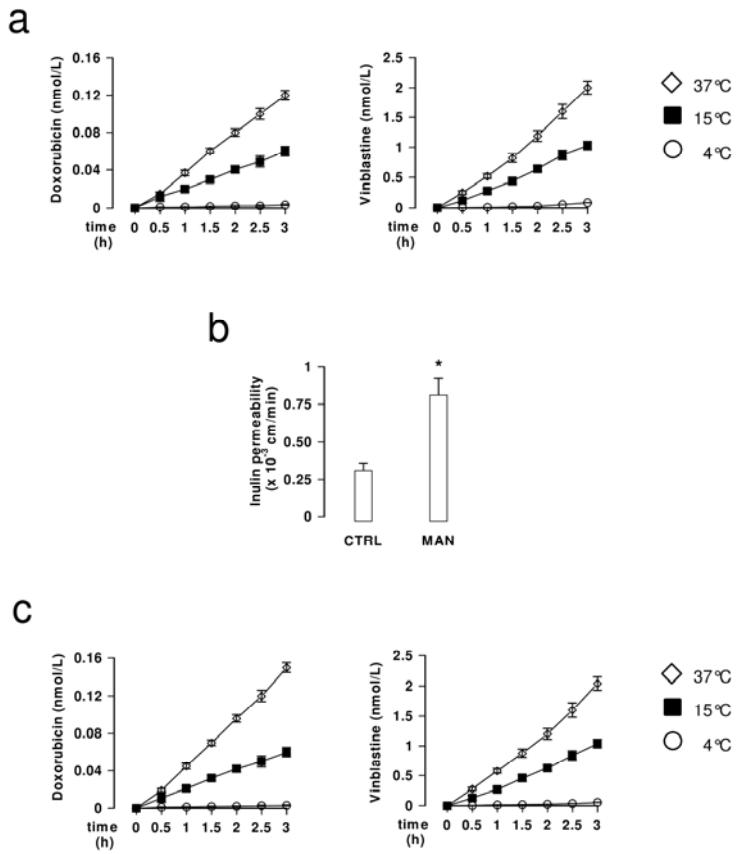

Online Resource 3. Time- and temperature-dependence in the transport of doxorubicin and vinblastine across hCMEC/D3 monolayer.

a. hCMEC/D3 cells were grown for 7 days up to confluence in Transwell inserts, then 5 µmol/L doxorubicin or 2 µCi/mL [^{3}H]-vinblastine (equivalent to 10.8 µmol/L) were added in the upper chamber. Plates were incubated at 4°C, 15°C and 37°C. From each plate, aliquots of 100 µL form the lower chamber medium were collected at fixed time point up to 3 h. The amount of the drug was measured fluorimetrically (for doxorubicin) or by liquid scintillation (for vinblastine). Measurements were performed in duplicate and data are presented as means ± SD (n = 3). **b.** hCMEC/D3 cells were grown for 7 days up to e confluence in Transwell inserts, then 2 µCi/mL [^{14}C]-inulin was added in the upper chamber, in the absence (*CTRL*) or presence of 25% w/v mannitol (*MAN*), chosen as tight junctions-disrupting agent. After 3 h the amount of inulin in the lower chamber was quantified by liquid scintillation. Measurements were performed in duplicate and data are presented as means ± SD (n = 2). Vs *CTRL*: * $p < 0.02$. **c.** hCMEC/D3 cells were treated as reported in **a**, in the presence of 25% w/v mannitol (*MAN*) in the upper chamber. The amount of the drug was measured fluorimetrically (for doxorubicin) or by liquid scintillation (for vinblastine). Measurements were performed in duplicate and data are presented as means ± SD (n = 3).

Online Resource 4

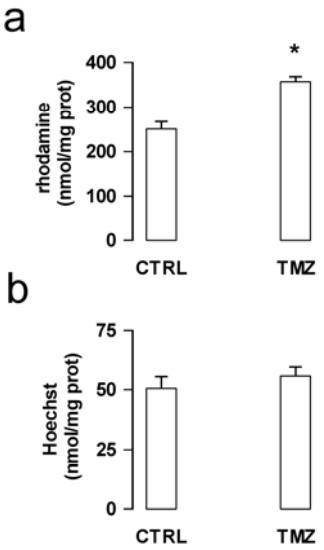

Online Resource 4. Intracellular accumulation of rhodamine 123 and Hoechst 33342 by hCMEC/D3 cells.

hCMEC/D3 cells were grown in fresh medium (*CTRL*) or with 50 μmol/L temozolomide (*TMZ*) for 72 h, then incubated with the Pgp/ABCB1 substrate rhodamine 123 (panel **a**) or the BCRP/ABCG2 substrate Hoechst 33342 (panel **b**). The intracellular retention of rhodamine 123 and Hoechst 33342 was measured in duplicate fluorimetrically, as reported under Materials and methods. Data are presented as means $\pm$ SD (n=4). Vs *CTRL*: * $p < 0.005$.

Online Resource 5

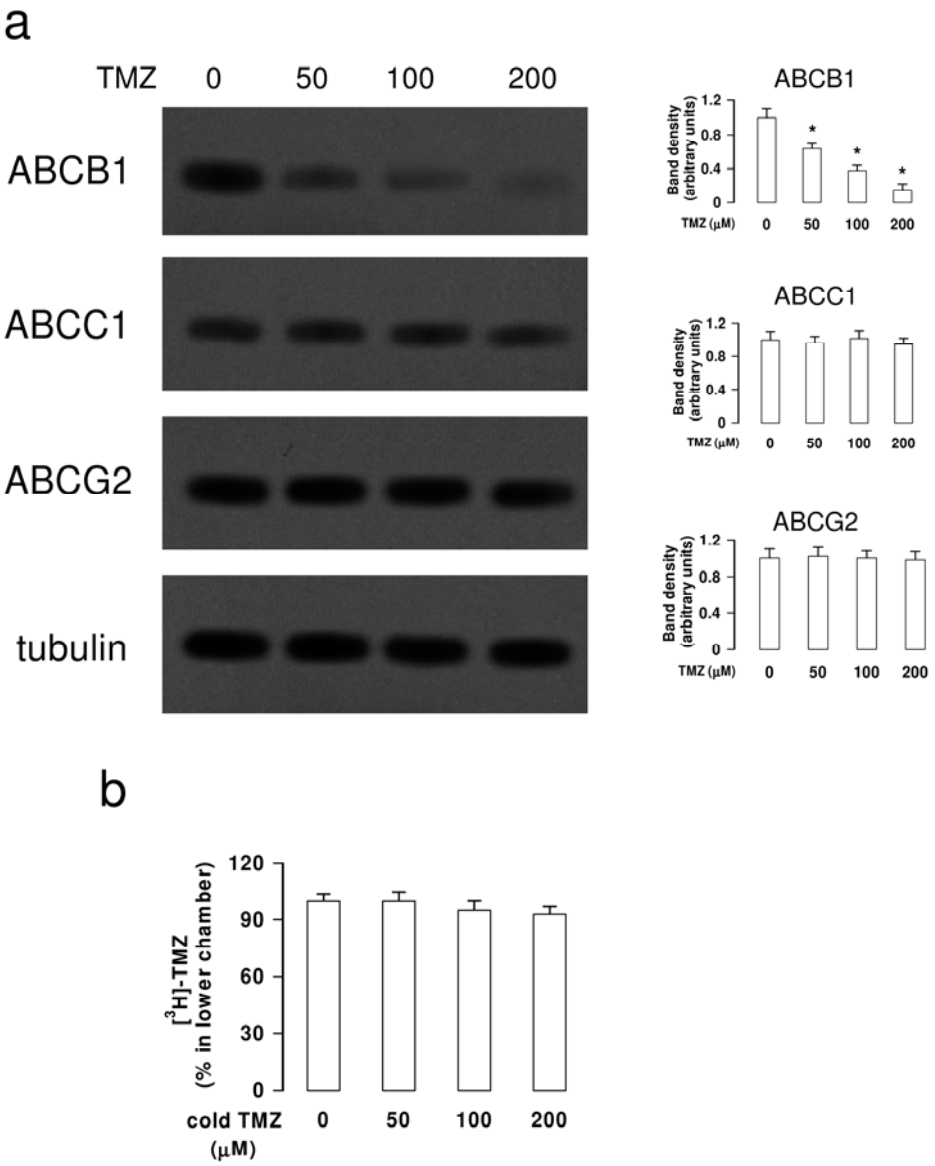

Online Resource 5. Effect of temozolomide on its own transport across hCMEC/D3 monolayer.

a. hCMEC/D3 cells were grown in fresh medium (*0*) or with 50, 100 or 200 μmol/L temozolomide (*TMZ*) for 72 h, then subjected to the Western blot analysis of Pgp/ABCB1, MRP1/ABCC1, BCRP/ABCG2. β-tubulin expression was used as control of equal protein loading. The figure is representative of 3 experiments with similar results. The band density ratio between each protein and β-tubulin was expressed as arbitrary units. Vs untreated cells (*0*): * $p < 0.05$. **b.** hCMEC/D3 cells were cultured in Transwell device for 7 days up to confluence, then incubated as reported in **a**, in the presence of 0.7 μC/mL (equivalent to 10 μmol/L) [^{3}H]-temozolomide. After this incubation period, the amount of [^{3}H]-temozolomide in the lower chamber was measured by liquid count scintillation. Results were expressed as percentage of [^{3}H]-temozolomide recovered in the lower chamber versus [^{3}H]-temozolomide added in the upper chamber at time 0. Data are presented as means $\pm$ SD (n=3).

Online Resource 6

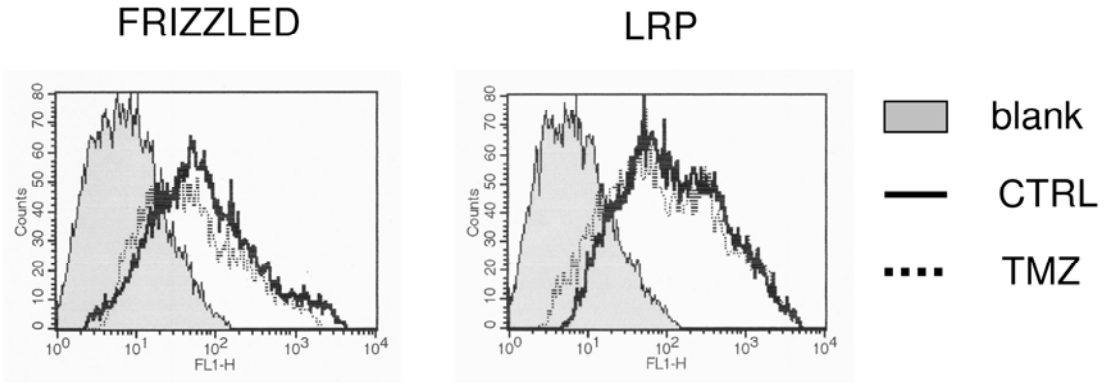

Online Resource 6. Effects of temozolomide on the expression of Frizzled and LRP6 in hCMEC/D3 cells.

hCMEC/D3 cells were incubated for 72 h in fresh medium (*CTRL*) or with 50 μmol/L temozolomide (*TMZ*). Flow cytometry analysis of surface Frizzled (left panel) and LRP6 (right panel) in cells untreated (*continuous line*) or treated with temozolomide (*dotted line*). *Grey peak*: cells treated with anti-isotypic antibody. The figures shown here are representative of 3 similar experiments, performed in triplicate.

Online Resource 7

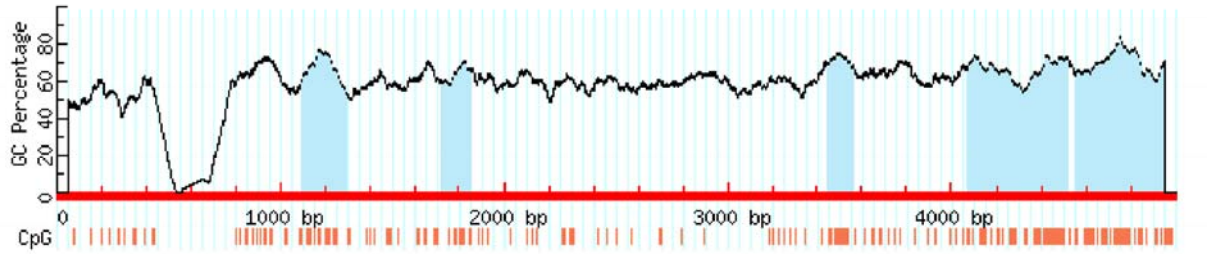

Online Resource 7. Localization of CpG islands on the promoter of *Wnt3* gene.

CpG islands localization on *Wnt3* promoter, according to Methprimer software (http://www.urogene.org/methprimer). As input the promoter sequence (from -5,000 bps to 0 bps) obtained by the UCSC Genome Browser (http://genome.ucsc.edu/) was used.

Online Resource 8

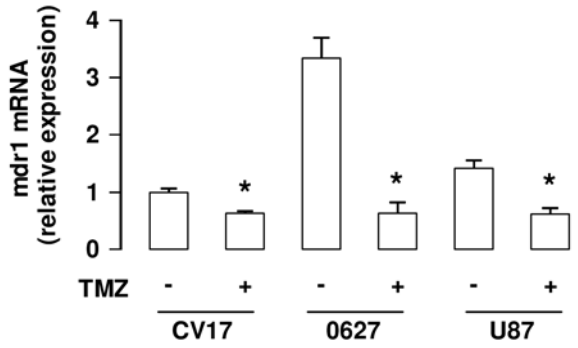

Online Resource 8. Effects of temozolomide on *mdr1* expression in glioblastoma cells co-cultured with hCMEC/D3 cells.

hCMEC/D3 cells were grown for 7 days up to confluence in Transwell inserts; CV17, 01010627 and U87-MG cells were seeded at day 4 in the lower chamber. After 3 days of co-culture, the supernatant in the upper chamber was replaced with fresh medium without (-) or with temozolomide (50 µmol/L for 48 h; *TMZ*). Total RNA was extracted and reverse-transcribed, the expression of *mdr1* gene was detected by qRT-PCR. The expression level in untreated CV17 cells was considered "1". Data are presented as means $\pm$ SD (n = 3). Vs untreated cells: * $p < 0.02$.

Online Resource 9

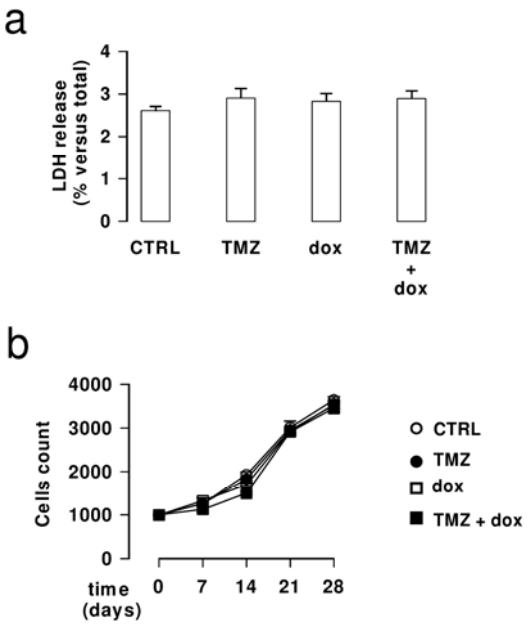

Online Resource 9. Effects of temozolomide and doxorubicin on cell survival of hCMEC/D3 cells.

a. hCMEC/D3 were cultured 7 days up to confluence, then incubated in fresh medium (CTRL), or medium containing 50 µmol/L temozolomide for 72 h (*TMZ*), 5 µmol/L doxorubicin for 24 h (*dox*), or 50 µmol/L temozolomide for 72 h plus 5 µmol/L doxorubicin in the last 24 h. The culture supernatant of cells was checked spectrophotometrically for the extracellular activity of LDH, taken as an index of cytotoxicity. Measurements were performed in duplicate and data are presented as means ± SD (n= 3). **b.** 1,000 hCMEC/D3 were seeded at day 0 in 96-wells plates. After 4 days, the medium was replaced with fresh medium (*open circles, CTRL*) or medium containing 50 µmol/L temozolomide for 72 h (*solid circles*, *TMZ*), 5 µmol/L doxorubicin for 24 h (*open squares*, *dox*), 50 µmol/L temozolomide for 72 h plus 5 µmol/L doxorubicin in the last 24 h (*solid squares*, *TMZ + dox*). Drug treatments were repeated every 7 days. Cell proliferation was monitored on day 7, 14, 21 and 28 by crystal violet staining. Measurements were performed in triplicate and data are presented as means ± SD (n= 3).

Online Resource 10

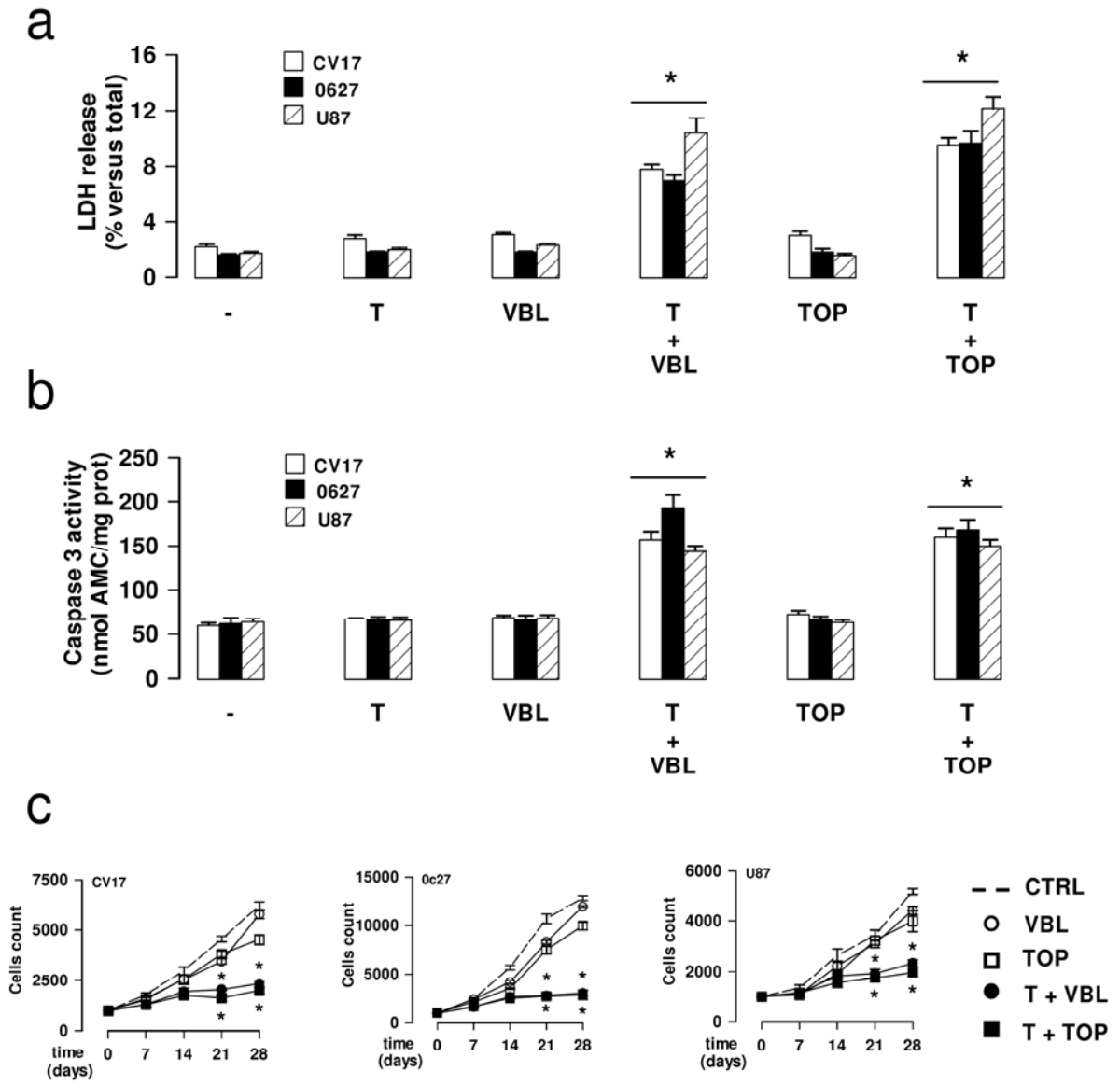

Online Resource 10. Effective cytotoxicity of the combination temozolomide plus vinblastine and topotecan on glioblastoma cells co-cultured with hCMEC/D3 cells.

hCMEC/D3 cells were grown for 7 days up to confluence in Transwell inserts; CV17, 01010627 and U87-MG cells were seeded at day 4 in the lower chamber. After 3 days of co-culture, the supernatant in the upper chamber was replaced with fresh medium without (-) or with temozolomide (50 µmol/L for 72 h; *T*). 20 nmol/L vinblastine (*VBL*) or 10 µmol/L topotecan (*TOP*) was added in the upper chamber of Transwell in the last 24 h, then the following investigations were performed. **a.** The culture supernatant of glioblastoma cells was checked for the extracellular activity of LDH. Measurements were performed in duplicate and data are presented as means $\pm$ SD (n= 4). Vs untreated cells: * $p < 0.02$. **b.** The activation of caspase-3 was measured fluorimetrically in glioblastoma cells lysates. Measurements were performed in duplicate and data are presented as means $\pm$ SD (n = 4). Vs untreated cells: * $p < 0.01$. **c.** After 3 days of co-culture, the medium of the upper chamber was replaced with fresh medium (*dashed line*) or medium containing 20 nmol/L vinblastine for 24 h (*open circles*, *VBL*), 10 µmol/L topotecan for 24 h (*open squares*, *TOP*), 50 µmol/L temozolomide for 72 h plus 20

nmol/L vinblastine in the last 24 h (*solid circles*, *T + VBL*), 50 µmol/L temozolomide for 72 h plus 10 µmol/L topotecan in the last 24 h (*solid squares*, *T + TOP*). Drug treatments were repeated every 7 days, as reported in the Materials and methods section. The proliferation of glioblastoma cells was monitored weekly by crystal violet staining. Measurements were performed in triplicate and data are presented as means $\pm$ SD (n= 4). Vs untreated cells (*CTRL*): * $p < 0.02$.

Online Resource 11

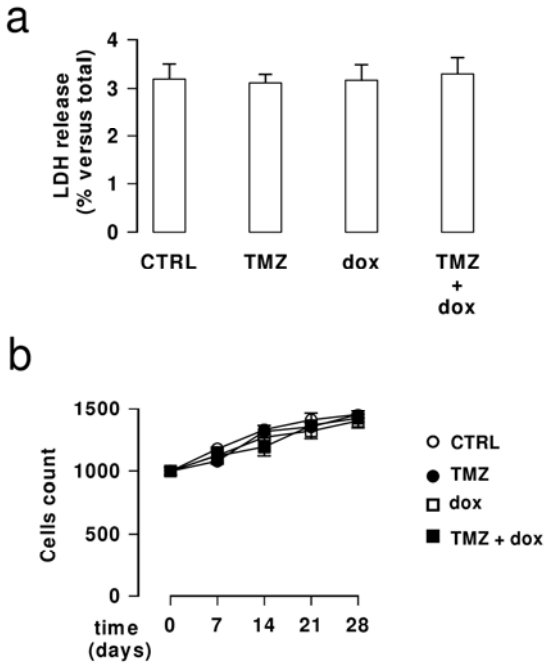

Online Resource 11. Effects of temozolomide and doxorubicin on cell survival of primary human brain microvascular endothelial cells.

a. HBMECs were cultured 7 days up to confluence, then incubated in fresh medium (CTRL), or medium containing 50 µmol/L temozolomide for 72 h (*TMZ*), 5 µmol/L doxorubicin for 24 h (*dox*), or 50 µmol/L temozolomide for 72 h plus 5 µmol/L doxorubicin in the last 24 h. The culture supernatant of cells was checked spectrophotometrically for the extracellular activity of LDH, taken as an index of cytotoxicity. Measurements were performed in duplicate and data are presented as means ± SD (n= 3). **b.** 1,000 HBMECs were seeded at day 0 in 96-wells plates. After 4 days, the medium was replaced with fresh medium (*open circles, CTRL*) or medium containing 50 µmol/L temozolomide for 72 h (*solid circles*, *TMZ*), 5 µmol/L doxorubicin for 24 h (*open squares*, *dox*), 50 µmol/L temozolomide for 72 h plus 5 µmol/L doxorubicin in the last 24 h (*solid squares*, *TMZ + dox*). Drug treatments were repeated every 7 days. Cell proliferation was monitored on day 7, 14, 21 and 28 by crystal violet staining. Measurements were performed in triplicate and data are presented as means ± SD (n= 3).